

W mass in a model with vector-like leptons and $U(1)'$

Junichiro Kawamura^{a 1} and Stuart Raby^{b 2}

^a *Center for Theoretical Physics of the Universe, Institute for Basic Science (IBS), Daejeon 34051, Korea*

^b *Department of Physics, Ohio State University, Columbus, Ohio, 43210, USA*

Abstract

We study the effects of vector-like leptons on the W boson mass in a model with a vector-like $U(1)'$ gauge symmetry. This model provides simultaneous explanations for the recent anomalies in the muon anomalous magnetic moment and the semi-leptonic decays of B mesons. We found that the recent result of the W boson mass precise measurement at CDF can be explained if the charged (neutral) vector-like lepton is lighter than 250 (80) GeV. The light vector-like leptons may not be excluded by collider experiments if these decay to a physical mode of the $U(1)'$ breaking scalar field.

¹jkawa@ibs.re.kr

²raby.1@osu.edu

1 Introduction

Recently, the CDF collaboration reported a new result of the precise W boson mass measurement [1],

$$m_W^{\text{CDF}} = 80.4335 (94) \text{ GeV}. \quad (1)$$

This value is larger than the combination of the previous measurements $m_W^{\text{PDG}} = 80.379 (12) \text{ GeV}$ and the Standard Model (SM) prediction $m_W^{\text{SM}} = 80.361 (6) \text{ GeV}$ [2]. Since the announcement of the result, the explanations for the new W boson mass and its relations to other physics have been studied extensively [3–77].

In this work, we point out that the shift of the W boson mass can be explained in a model with vector-like (VL) leptons and an extra $U(1)'$ gauge symmetry which was proposed in Refs. [78, 79]. The model provides a simultaneous explanation for the anomalies in the muon anomalous magnetic moment, $g-2$, and the semi-leptonic decays of the B meson³. The recent FNAL measurement [97] confirmed the long-standing discrepancy of the muon $g-2$ between the experimental value [98] and the SM prediction [99–118], and the current discrepancy is $\Delta a_\mu = 2.51 (59) \times 10^{-9}$. Yet another discrepancy from the SM is found in the measurements of rare semi-leptonic B meson decays [119–135], $b \rightarrow s\ell\ell$. In this paper, we focus on the VL leptons and Z' boson in this model to show that m_W and Δa_μ can be explained simultaneously. As we have shown in Refs. [78, 79], this model can easily accommodate the $b \rightarrow s\ell\ell$ anomaly when the Z' boson is sufficiently light and strongly couples to muons, so that Δa_μ is explained. Therefore, our model will provide a unified explanation for the recent three anomalies, m_W , Δa_μ and $b \rightarrow s\ell\ell$. It will turn out that the VL leptons should be lighter than those to explain Δa_μ . Hence we will study the observables which would be changed from the SM values due to the light VL leptons.

The rest of this paper is organized as follows. The model is briefly introduced in Sec. 2, and then the observables in our analysis are discussed in Sec. 3. The result of a numerical analysis is shown and the LHC signals are discussed in Sec. 4. Section 5 is devoted to summary. Diagonalization of the mass matrices is discussed in Appendix A, and the formula for the three-body decays are shown in Appendix B.

2 Model

2.1 Mass matrices

We briefly introduce our model, with particular interests in VL leptons, see Refs. [78, 79] for more details. The matter content relevant to the discussion in this work is shown in Table 1. We assume that the VL leptons mix with only the SM leptons in the second generation to prevent

³Models with VL fermions and a $U(1)'$ symmetry for the anomalies are proposed in Refs. [80–90]. Explanations for Δa_μ by VL leptons are proposed in e.g. Refs. [91–96].

Table 1: Matter contents. Electric charge of fermion f is $Q_f = T_f^3 + Y_f/2$. The $SU(2)_L$ doublets have components; $\ell_L = (\nu_L, \mu_L)$, $H = (H_0, H_-)$, $L_L = (N'_L, E'_L)$ and $\bar{L}_R = (-\bar{E}'_R, \bar{N}'_R)$.

	ℓ_L	$\bar{\mu}_R$	$\bar{\nu}_R$	H	L_L	\bar{E}_R	\bar{L}_R	E_L	N_L	\bar{N}_R	Z'	Φ
$SU(2)_L$	2	1	1	2	2	1	2	1	1	1	1	1
$U(1)_Y$	-1	2	0	-1	-1	2	1	-2	0	0	0	0
$U(1)'$	0	0	0	0	-1	1	1	-1	-1	1	0	-1

flavor violations. The mass terms and the Yukawa couplings are given by

$$\begin{aligned} \mathcal{L} \supset & -m_L \bar{L}_R L_L - m_E \bar{E}_R E_L - m_N \bar{N}_R N_L - \frac{1}{2} M_R \bar{\nu}_R^c \nu_R \\ & + y_2 \bar{\mu}_R \ell_L H + y_n \bar{\nu}_R \ell_L \tilde{H} + \lambda_L \Phi \bar{L}_R \ell_L - \lambda_E \Phi^* \bar{\mu}_R E_L - \lambda_N \Phi^* \bar{\nu}_R N_L \\ & + \lambda_e \bar{E}_R L_L H - \lambda'_e \bar{L}_R \tilde{H} E_L + \lambda_n \bar{N}_R L_L \tilde{H} + \lambda'_n \bar{L}_R H N_L + h.c., \end{aligned} \quad (2)$$

where $\tilde{H} := i\sigma_2 H^* = (H_-^*, -H_0^*)$. The $SU(2)_L$ indices are contracted by $i\sigma_2$. We introduce the Majorana mass term of ν_R for the type-I see-saw mechanism. After the scalar fields develop their vacuum expectation values (VEVs), $v_H := \langle H_0 \rangle$ and $v_\Phi := \langle \Phi \rangle$, the Dirac mass matrices for the leptons are given by

$$\bar{\mathbf{e}}_R \mathcal{M}_e \mathbf{e}_L := \begin{pmatrix} \bar{\mu}_R & \bar{E}_R & \bar{E}'_R \end{pmatrix} \begin{pmatrix} y_2 v_H & 0 & \lambda_E v_\Phi \\ 0 & \lambda_e v_H & m_E \\ \lambda_L v_\Phi & m_L & \lambda'_e v_H \end{pmatrix} \begin{pmatrix} \mu_L \\ E'_L \\ E_L \end{pmatrix}, \quad (3)$$

$$\bar{\mathbf{n}}_R \mathcal{M}_n \mathbf{n}_L := \begin{pmatrix} \bar{\nu}_R & \bar{N}_R & \bar{N}'_R \end{pmatrix} \begin{pmatrix} y_n v_H & 0 & \lambda_N v_\Phi \\ 0 & \lambda_n v_H & m_N \\ \lambda_L v_\Phi & m_L & \lambda'_n v_H \end{pmatrix} \begin{pmatrix} \nu_L \\ N'_L \\ N_L \end{pmatrix}. \quad (4)$$

The mass basis is defined as

$$\hat{\mathbf{e}}_L := U_{e_L}^\dagger \mathbf{e}_L, \quad \hat{\mathbf{e}}_R := U_{e_R}^\dagger \mathbf{e}_R, \quad \hat{\mathbf{n}}_L := U_{n_L}^\dagger \mathbf{n}_L, \quad \hat{\mathbf{n}}_R := U_{n_R}^\dagger \mathbf{n}_R, \quad (5)$$

where unitary matrices diagonalize the mass matrices as

$$U_{e_R}^\dagger \mathcal{M}_e U_{e_L} = \begin{pmatrix} m_\mu & 0 & 0 \\ 0 & m_{E_1} & 0 \\ 0 & 0 & m_{E_2} \end{pmatrix}, \quad U_{n_R}^\dagger \mathcal{M}_n U_{n_L} = \begin{pmatrix} \cdot & \cdot & \cdot \\ 0 & m_{N_1} & 0 \\ 0 & 0 & m_{N_2} \end{pmatrix}. \quad (6)$$

The masses are increasingly ordered. Here, \cdot 's in the first row of the neutrino mass matrix will be irrelevant after ν_R is integrated out. Neglecting $\mathcal{O}(v_H)$ entries, the VL lepton masses are given by

$$m_{E_1} \sim M_E := \sqrt{m_E^2 + \lambda_E^2 v_\Phi^2}, \quad m_{N_1} \sim m_N, \quad m_{E_2} \sim m_{N_2} \sim M_L := \sqrt{m_L^2 + \lambda_L^2 v_\Phi^2}, \quad (7)$$

when $M_E, m_N < M_L$ and hence $L \sim (E_2, N_2)$.

We define the Dirac fermions as

$$\hat{\mathbf{e}} := (\mu, E_1, E_2), \quad \hat{\mathbf{n}} := (\nu, N_1, N_2), \quad (8)$$

where

$$[\mathbf{e}]_i := ([\hat{\mathbf{e}}_L]_i, [\hat{\mathbf{e}}_R]_i), \quad [\mathbf{n}]_i := ([\hat{\mathbf{n}}_L]_i, [\hat{\mathbf{n}}_R]_i), \quad (9)$$

with $i = 1, 2, 3$. We expand the neutral scalar fields as

$$H_0 = v_H + \frac{1}{\sqrt{2}}(h + ia_h), \quad \Phi = v_\Phi + \frac{1}{\sqrt{2}}(\chi + ia_\chi), \quad (10)$$

where h and χ are the physical real scalar fields, while the pseudo-scalar components a_h and a_χ are absorbed by the Z and Z' bosons, respectively.

2.2 Interactions

The Z and W boson couplings are given by

$$\mathcal{L}_{Z,W} = Z_\mu \sum_{f=\mathbf{e},\mathbf{n}} \bar{f} \gamma^\mu (g_{fL}^Z P_L + g_{fR}^Z P_R) f + \left[W_\mu \bar{\mathbf{n}} \gamma^\mu (g_L^W P_L + g_R^W P_R) \mathbf{e} + h.c. \right], \quad (11)$$

where

$$g_{\mathbf{e}A}^Z = \frac{g}{2c_W} (-\mathcal{E}^A + 2s_W^2 \mathbf{1}_3), \quad g_{\mathbf{n}A}^Z = \frac{g}{2c_W} \mathcal{N}^A, \quad g_A^W = \frac{g}{\sqrt{2}} h^A, \quad (12)$$

for $A = L, R$. Here,

$$\mathcal{E}^A := U_{eA}^\dagger Q_A U_{eA}, \quad \mathcal{N}^A := U_{nA}^\dagger Q_A U_{nA}, \quad h^A := U_{nA}^\dagger Q_A U_{eA}, \quad (13)$$

where $Q_L = \text{diag}(1, 1, 0)$ and $Q_R = \mathbf{1}_3 - Q_L$. P_L (P_R) are the chiral projections onto the left- (right-) handed fermions.

The gauge interactions with the Z' boson in the mass basis are defined as

$$\mathcal{L}_{Z'} = Z'_\mu \sum_{f=\mathbf{e},\mathbf{n}} \bar{f} \gamma^\mu (g_{fL}^{Z'} P_L + g_{fR}^{Z'} P_R) f, \quad (14)$$

where the coupling matrices are given by

$$g_{\mathbf{e}A}^{Z'} = g' U_{eA}^\dagger Q'_e U_{eA}, \quad g_{\mathbf{n}A}^{Z'} = g' U_{nA}^\dagger Q'_n U_{nA}, \quad (15)$$

with $Q'_e = Q'_n = \text{diag}(0, -1, -1)$. g' is the gauge coupling constant for $U(1)'$.

The Yukawa interactions are given by

$$-\mathcal{L}_Y = \frac{1}{\sqrt{2}} \sum_{S=h,\chi} \sum_{f=\mathbf{e},\mathbf{n}} S \bar{f} Y_f^S P_L f + h.c., \quad (16)$$

where

$$Y_{\mathbf{e}}^h = U_{e_R}^\dagger \begin{pmatrix} y_2 & 0 & 0 \\ 0 & \lambda_e & 0 \\ 0 & 0 & \lambda'_e \end{pmatrix} U_{e_L}, \quad Y_{\mathbf{e}}^X = U_{e_R}^\dagger \begin{pmatrix} 0 & 0 & \lambda_E \\ 0 & 0 & 0 \\ \lambda_L & 0 & 0 \end{pmatrix} U_{e_L}, \quad (17)$$

$$Y_{\mathbf{n}}^h = U_{n_R}^\dagger \begin{pmatrix} y_n & 0 & 0 \\ 0 & \lambda_n & 0 \\ 0 & 0 & \lambda'_n \end{pmatrix} U_{n_L}, \quad Y_{\mathbf{n}}^X = U_{n_R}^\dagger \begin{pmatrix} 0 & 0 & \lambda_N \\ 0 & 0 & 0 \\ \lambda_L & 0 & 0 \end{pmatrix} U_{n_L}. \quad (18)$$

2.3 Couplings at the leading order

We show the structures of the coupling matrices at the leading order in $\mathcal{O}(m_\mu/v_\Phi)$. Hereafter, we assume $\lambda_e, \lambda_n \sim y_2$, so that the muon mass is explained without fine-tuning, and the Z and W boson couplings to the SM leptons do not sizably deviate from the SM values. The formulas with the sub-leading terms are explicitly shown in Appendix A. The Z' couplings are given by

$$g_{\mathbf{e}_L}^{Z'} = g' U_L^\dagger Q'_L U_L \sim -g' \begin{pmatrix} s_L^2 & -c_L s_L c_{e_L} & c_L s_L s_{e_L} \\ -c_L s_L c_{e_L} & s_{e_L}^2 + c_L^2 c_{e_L}^2 & s_L^2 s_{e_L} c_{e_L} \\ c_L s_L s_{e_L} & s_L^2 s_{e_L} c_{e_L} & c_L^2 s_{e_L}^2 + c_{e_L}^2 \end{pmatrix}, \quad (19)$$

$$g_{\mathbf{e}_R}^{Z'} = g' U_R^\dagger Q'_R U_R \sim -g' \begin{pmatrix} s_E^2 & -c_E s_E s_{e_R} & -c_E s_E c_{e_R} \\ -c_E s_E s_{e_R} & c_{e_R}^2 + c_E^2 s_{e_R}^2 & -s_E^2 s_{e_R} c_{e_R} \\ -c_E s_E c_{e_R} & -s_E^2 s_{e_R} c_{e_R} & c_E^2 c_{e_R}^2 + s_{e_R}^2 \end{pmatrix}, \quad (20)$$

where

$$c_X := \frac{m_X}{M_X}, \quad s_X := \frac{\lambda_X v_\Phi}{M_X}, \quad X = L, E. \quad (21)$$

Here, c_{e_A} and s_{e_A} ($A = L, R$) are the angles to diagonalize the VL mass matrix, defined in Eq. (60). These are approximately given by

$$c_{e_A} \simeq 1 - \frac{\eta_{e_A}^2}{2}, \quad s_{e_A} \simeq \eta_{e_A}, \quad \eta_{e_L} := \frac{\lambda'_e v_H M_L}{M_L^2 - M_E^2}, \quad \eta_{e_R} := \frac{\lambda'_e v_H M_E}{M_L^2 - M_E^2}, \quad (22)$$

for $\eta_{e_A} \ll 1$. Those for the neutrino couplings $g_{\mathbf{n}_A}^{Z'}$ are given by replacing $s_E \rightarrow 0$, $c_E \rightarrow 1$ and $e_A \rightarrow n_A$. The isospin parts of the Z and W boson couplings are given by

$$\mathcal{E}^A \sim \begin{pmatrix} \delta_{AL} & 0 & 0 \\ 0 & c_{e_A}^2 & -c_{e_A} s_{e_A} \\ 0 & -c_{e_A} s_{e_A} & s_{e_A}^2 \end{pmatrix}, \quad \mathcal{N}^A \sim \begin{pmatrix} \delta_{AL} & 0 & 0 \\ 0 & c_{n_A}^2 & -c_{n_A} s_{n_A} \\ 0 & -c_{n_A} s_{n_A} & s_{n_A}^2 \end{pmatrix}, \quad (23)$$

and

$$h^A \sim \begin{pmatrix} \delta_{AL} & 0 & 0 \\ 0 & c_{eA}c_{nA} & -c_{nA}s_{eA} \\ 0 & -c_{eA}s_{nA} & s_{eA}s_{nA} \end{pmatrix}, \quad (24)$$

for $A = L, R$. Here, $\delta_{AL} = 1$ (0) for $A = L$ (R). Thus, the SM lepton couplings to the Z and W bosons are the same as the SM ones, and the off-diagonal couplings of the SM and VL fermions are vanishing, up to $\mathcal{O}(m_\mu/v_\Phi)$. This is in contrast to the model studied in Ref. [20], and hence the W -mass could be addressed in this model solely by the VL leptons.

The Yukawa couplings to the scalars h and χ are respectively given by

$$Y_e^h \sim \begin{pmatrix} y_2 c_L c_E + \lambda_e s_L s_E & \mathcal{O}(y_2) & \mathcal{O}(y_2) \\ \mathcal{O}(y_2) & s_{eL} c_{eR} \lambda'_e & c_{eL} c_{eR} \lambda'_e \\ \mathcal{O}(y_2) & -s_{eL} s_{eR} \lambda'_e & -c_{eL} s_{eR} \lambda'_e \end{pmatrix}, \quad (25)$$

$$Y_e^\chi \sim \begin{pmatrix} 0 & c_E s_{eL} \lambda_E & c_E c_{eL} \lambda_E \\ c_L c_{eR} \lambda_L & s_E s_{eL} s_{eR} \lambda_E + s_L c_{eL} c_{eR} \lambda_L & s_E c_{eL} s_{eR} \lambda_E - s_L s_{eL} c_{eR} \lambda_L \\ -c_L s_{eR} \lambda_L & s_E s_{eL} c_{eR} \lambda_E - s_L c_{eL} s_{eR} \lambda_L & s_E c_{eL} c_{eR} \lambda_E + s_L s_{eL} s_{eR} \lambda_L \end{pmatrix}. \quad (26)$$

Those for the neutrinos are given by replacing $y_2 \rightarrow 0$, $e \rightarrow n$ and $E \rightarrow N$. Note that $m_\mu \sim (y_2 c_L c_E + \lambda_e s_L s_E) v_H$, so the Yukawa coupling to the Higgs boson is also not changed from the SM value for heavy VL leptons. The SM Higgs couplings to the SM and VL leptons are again suppressed by the small muon Yukawa coupling. The χ boson coupling to the SM muon vanishes if we neglect the muon mass.

3 Phenomenology

3.1 Oblique parameters and W boson mass

In this model, the VL lepton contributions to the T parameter, one of the oblique parameters [136, 137], is given by [138],

$$16\pi s_W^2 c_W^2 T = \sum_{a,\beta} \left\{ \left(|h_{a\beta}^L|^2 + |h_{a\beta}^R|^2 \right) \theta_+(y_a, y_\beta) + 2\text{Re} \left(h_{a\beta}^L h_{a\beta}^{R*} \right) \theta_-(y_a, y_\beta) \right\} \quad (27)$$

$$- \sum_{a < b} \left\{ \left(|\mathcal{N}_{ab}^L|^2 + |\mathcal{N}_{ab}^R|^2 \right) \theta_+(y_a, y_b) + 2\text{Re} \left(\mathcal{N}_{ab}^L \mathcal{N}_{ab}^{R*} \right) \theta_-(y_a, y_b) \right\}$$

$$- \sum_{\alpha < \beta} \left\{ \left(|\mathcal{E}_{\alpha\beta}^L|^2 + |\mathcal{E}_{\alpha\beta}^R|^2 \right) \theta_+(y_\alpha, y_\beta) + 2\text{Re} \left(\mathcal{E}_{\alpha\beta}^L \mathcal{E}_{\alpha\beta}^{R*} \right) \theta_-(y_\alpha, y_\beta) \right\},$$

where $a, b = 1, 2, 3$ ($\alpha, \beta = 1, 2, 3$) run over the neutral (charged) leptons. These subscripts are the elements of the couplings matrices, e.g. $h_{a\beta}^L := [h^L]_{a\beta}$. The other oblique parameters, $2\pi S$

and $-2\pi U$, are obtained by replacing the functions, $\theta_{\pm} \rightarrow \chi_{\pm}$, except for the first line in the S parameter which should be replaced as $\theta_{\pm} \rightarrow \psi_{\pm}$. The loop functions are defined in Ref. [41]. For an order of magnitude estimation, taking $s_{e_A}, s_{n_A} = 0$ and $m_{L^0} \simeq m_{L^-}$, we have

$$16\pi s_W^2 c_W^2 T \sim \frac{2(m_{L^-}^2 - m_{L^0}^2)^2}{3m_Z^2 M_L^2} \sim \frac{2v_H^4}{3m_Z^2 M_L^2} \left(\frac{\lambda_e'^2}{1 - M_E^2/M_L^2} - \frac{\lambda_n'^2}{1 - m_N^2/M_L^2} \right)^2, \quad (28)$$

where m_{L^-} and m_{L^0} are the masses of doublet-like charged and neutral VL leptons, respectively. $\eta_{e_A}, \eta_{n_A} \ll 1$ is assumed in the second equality. Hence,

$$T \sim 0.13 \times \left(\frac{\lambda_e'^2}{1 - M_E^2/M_L^2} - \frac{\lambda_n'^2}{1 - m_N^2/M_L^2} \right)^2 \left(\frac{250 \text{ GeV}}{M_L} \right)^2, \quad (29)$$

where we used $s_W^2 = 0.23121$ [2]. The W boson mass is related to the oblique parameters as [139, 140]⁴

$$\frac{\delta m_W^2}{m_W^2|_{\text{SM}}} = \frac{\alpha_e}{c_W^2 - s_W^2} \left(-\frac{1}{2}S + c_W^2 T + \frac{c_W^2 - s_W^2}{4s_W^2} U + \frac{s_W^2}{\alpha_e} \epsilon_{\mu} \right) \sim 0.001 \times \left(\frac{T}{0.1} \right), \quad (30)$$

where $T \gg S, U$ and $\epsilon_{\mu} \simeq 0$ are assumed in the second equality. We include the shift from the W boson coupling to the muon at tree-level, $h_{11}^L =: h_{\nu\mu}^L =: 1 - \epsilon_{\mu}$. Hereafter, we write the indices for the SM leptons by ν/μ instead of 1, so that these are not confused with the first generations. Note that ϵ_{μ} is positive in our model as shown in Eq. (61). Therefore, from Eq. (29), the shift may be explained if $\lambda_e', \lambda_n' \sim \mathcal{O}(1)$, $M_L \sim 250 \text{ GeV}$ and $M_E^2/M_L^2, m_N^2/M_L^2$ are $\mathcal{O}(1)$.

3.2 Muon $g - 2$

The muon anomalous magnetic moment Δa_{μ} is shifted by the 1-loop effects via the Z' and χ bosons. This is approximately given by [93, 141]

$$\Delta a_{\mu} \sim -\frac{m_{\mu} \lambda_e' v_H}{16\pi^2 m_{Z'}^2} \tilde{C}_{LR}, \quad (31)$$

$$\tilde{C}_{LR} := \frac{\lambda_L \lambda_E m_L m_E}{M_L M_E} \left(\frac{G_Z(x_L) - G_Z(x_E)}{x_L - x_E} + \frac{m_{Z'}^2}{2m_{\chi}^2} \frac{y_L G_S(y_L) - y_R G_S(y_R)}{y_L - y_R} \right), \quad (32)$$

where $x_L := M_L^2/m_{Z'}^2$, $x_E := M_E^2/m_{Z'}^2$, $y_L := M_L^2/m_{\chi}^2$ and $y_E := M_E^2/m_{\chi}^2$. The exact formula and the loop functions are shown in Refs. [78, 79]. The value of Δa_{μ} is estimated as

$$\Delta a_{\mu} \sim 5 \times 10^{-9} \times \lambda_e' \left(\frac{500 \text{ GeV}}{m_{Z'}} \right)^2 \left(\frac{\tilde{C}_{LR}}{-0.01} \right). \quad (33)$$

Hence, the Z' boson with mass of order 500 GeV can explain Δa_{μ} .

⁴We neglect the difference in the definitions of the oblique parameters. The length of slopes of self-energies are taken to be finite value [138], but these effects are less than 5% in the parameter space studied in this paper, and thus not important.

3.3 EW observables

The mixing of the second generation leptons and the VL states can change the SM predictions of the EW boson couplings. The Fermi constant G_μ determined by the muon decay is given by

$$G_\mu = G_F |h_{\nu\mu}^L|, \quad \frac{G_F}{\sqrt{2}} = \frac{g^2}{8m_W^2}, \quad (34)$$

at the tree-level, where $G_\mu = 1.1663787 \times 10^{-5} \text{ GeV}^2$ [2]. The partial width of the W boson is given by

$$\text{BR}(W \rightarrow \mu\nu) = \frac{g^2 m_W}{48\pi\Gamma_W} |h_{\nu\mu}^L|^2, \quad (35)$$

where the muon and neutrino masses are neglected. In the SM, the gauge coupling constant and Γ_W are given by $g(m_Z) = 0.65184$ (18) [142] and $\Gamma_W = 2.0895$ (8) GeV [143], respectively. We use these SM values for numerical analysis, since the branching fraction, $\propto g^2 m_W / \Gamma_W$, is approximately independent of g and m_W .

The Z boson partial decay widths are given by

$$\Gamma(Z \rightarrow \mu\mu) = \frac{G_F m_Z^3}{12\sqrt{2}\pi} \left(1 + \frac{3\alpha_e}{4\pi}\right) \left(|-\mathcal{E}_{\mu\mu}^L + 2s_W^2|^2 + |-\mathcal{E}_{\mu\mu}^R + 2s_W^2|^2\right), \quad (36)$$

$$\Gamma(Z \rightarrow \text{inv}) = \frac{G_F m_Z^3}{12\sqrt{2}\pi} \left(2 + |\mathcal{N}_{\nu\nu}^L|^2\right), \quad (37)$$

where the Z boson couplings to the electron and tau neutrinos are set to the SM values. The leading QED effect is included for $Z \rightarrow \mu\mu$. The asymmetry parameter A_μ and A_{FB}^μ are given by

$$A_\mu = \frac{(\mathcal{E}_{\mu\mu}^L)^2 - (\mathcal{E}_{\mu\mu}^R)^2 - 4s_W^2 (\mathcal{E}_{\mu\mu}^L - \mathcal{E}_{\mu\mu}^R)}{(\mathcal{E}_{\mu\mu}^L)^2 + (\mathcal{E}_{\mu\mu}^R)^2 - 4s_W^2 (\mathcal{E}_{\mu\mu}^L + \mathcal{E}_{\mu\mu}^R) + 8s_W^4}, \quad A_{FB}^\mu = \frac{3}{4} A_e A_\mu. \quad (38)$$

Since the Z boson couplings to the electrons are the SM-like, $A_e = A_e^{\text{SM}} = 0.1468$ (03) [2]. We shall use the SM value for the weak angle, $s_W^2 = 0.23155$ [2] to calculate A_μ .

Similarly to the SM gauge bosons, $h \rightarrow \mu\mu$ can deviate from the SM value. We define the ratio of the width,

$$R_{\mu\mu} := \frac{\Gamma(h \rightarrow \mu\mu)}{\Gamma(h \rightarrow \mu\mu)_{\text{SM}}} = \frac{v_H^2}{m_\mu^2} \left| [Y_e^h]_{\mu\mu} \right|^2. \quad (39)$$

The decay rate of $h \rightarrow \gamma\gamma$ will deviate from the SM value due to the loop effects mediated by the charged VL leptons. We define the ratio of the width of $h \rightarrow \gamma\gamma$ to that in the SM as

$$R_{\gamma\gamma} := \frac{\Gamma(h \rightarrow \gamma\gamma)}{\Gamma(h \rightarrow \gamma\gamma)_{\text{SM}}} = \left| 1 + \sum_{i=1,2} \left([Y_e^h]_{E_i E_i} \frac{v_H}{m_{E_i}} \right) \frac{A_{1/2}^H(\tau_{E_i})}{A_{\text{SM}}} \right|^2, \quad (40)$$

where $\tau_I = m_H^2/(4m_I^2)$ for the lower case $I = E_1, E_2$, and the SM contribution A_{SM} is given by [144]

$$A_{\text{SM}} := A_1^H(\tau_W) + \sum_f N_c^f Q_f^2 A_{1/2}^H(\tau_f). \quad (41)$$

Here, f runs over all the SM fermions. Q_f and N_c^f are the electric charge and the number of colors of the fermion f , respectively. Assuming that the production cross sections are the same as in the SM, the current experimental values are $R_{\mu\mu} = 1.19 \pm 0.34$ and $R_{\gamma\gamma} = 1.10 \pm 0.07$ [2].

For $h_{\nu\mu}^L \neq 1$, the SM gauge boson couplings are not lepton flavor universal. We shall consider the decays of Z , W bosons and τ ,

$$\frac{\Gamma(Z \rightarrow \mu\mu)}{\Gamma(Z \rightarrow ee)} = \frac{|-\mathcal{E}_{\mu\mu}^L + 2s_W^2|^2 + |-\mathcal{E}_{\mu\mu}^R + 2s_W^2|^2}{1 - 4s_W^2 + 8s_W^4}, \quad \frac{\Gamma(W \rightarrow \mu\nu)}{\Gamma(W \rightarrow e\nu)} = |h_{\nu\mu}^L|^2, \quad (42)$$

$$\frac{\Gamma(\tau \rightarrow \mu\nu\nu)}{\Gamma(\tau \rightarrow e\nu\nu)} = |h_{\nu\mu}^L|^2 F_\ell \left(\frac{m_\mu^2}{m_\tau^2} \right), \quad (43)$$

where

$$F_\ell(y) = 1 - 8y + 8y^3 - y^4 - 12y^2 \log y. \quad (44)$$

We also study the ratio of the Z/W boson decays to tau and muon, $\Gamma(Z \rightarrow \tau\tau)/\Gamma(Z \rightarrow \mu\mu)$ and $\Gamma(W \rightarrow \tau\nu)/\Gamma(W \rightarrow \mu\nu)$ which are given by the inverse of Eq. (42) in our model.

3.4 Muon trident process

The Z' boson can induce the so-called neutrino trident process, $\nu_\mu N \rightarrow \nu_\mu \mu^+ \mu^- N$ [145–150]. The cross section for this process at the CCFR experiment is estimated as [150, 151]

$$R_{\text{CCFR}} := \frac{\sigma_{\text{CCFR}}}{\sigma_{\text{CCFR}}^{\text{SM}}} \simeq \frac{(1 + 4s_W^2 + \Delta g_{\mu\mu\mu\mu}^V)^2 + 1.13(1 - \Delta g_{\mu\mu\mu\mu}^A)^2}{(1 + 4s_W^2)^2 + 1.13}, \quad (45)$$

where the Z' boson contributions $\Delta g_{\mu\mu\mu\mu}^{V,A}$ are given by

$$\Delta g_{\mu\mu\mu\mu}^{V,A} = \frac{\sqrt{2}}{G_F \cdot 2m_{Z'}^2} [g_{\mathbf{n}_L}^{Z'}]_{\nu_\mu\nu_\mu} \left([g_{\mathbf{e}_R}^{Z'}]_{\mu\mu} \pm [g_{\mathbf{e}_L}^{Z'}]_{\mu\mu} \right) \sim \frac{s_L^2 (s_E^2 \pm s_L^2)}{2\sqrt{2}G_F v_\Phi^2}. \quad (46)$$

The experimentally observed rate is $\sigma_{\text{CCFR}}/\sigma_{\text{CCFR}}^{\text{SM}} = 0.82 \pm 0.28$ at 95% C.L.⁵

3.5 $b \rightarrow s\mu\mu$ anomaly

We emphasize that the recent anomaly in the $b \rightarrow s\ell\ell$ process can easily be explained in this model. The Wilson coefficients for the semi-leptonic operators are given by

$$C_{9,10} \sim -\frac{\pi}{2\sqrt{2}\alpha_e G_F} \frac{1}{V_{tb}V_{ts}^*} \left(\frac{\lambda_E^2}{M_E^2} \pm \frac{\lambda_L^2}{M_L^2} \right) \frac{g_{sb}^{Z'}}{g'}, \quad (47)$$

⁵For the calculation of R_{CCFR} , we used $s_W^2 = 0.23129$ as in Ref. [150].

where V_{tb} and V_{ts} are the CKM elements, and $g_{sb}^{Z'}$ is the Z' boson coupling constant to sb in the left-handed interaction. The Wilson coefficient C_9 is estimated as

$$C_9 \sim -0.8 \times \left(\frac{200 \text{ GeV}}{m_{\text{VLL}}} \right)^2 \left(\frac{g_{sb}^{Z'}/g'}{10^{-4}} \right), \quad \frac{1}{m_{\text{VLL}}^2} := \frac{\lambda_E^2}{M_E^2} + \frac{\lambda_L^2}{M_L^2}, \quad (48)$$

whereas the current favored values is $C_9 \in [-1.0, -0.5]$ depending on the value of C_{10} [152–158]. Thus, the $b \rightarrow s\ell\ell$ anomaly can be explained even with the small Z' coupling to quarks, as long as those to the VL leptons are sizable to explain the shift in m_W and Δa_μ . With such small couplings to the Z' boson, the flavor violations such as B_s - \bar{B}_s mixing will not deviate from the SM prediction due to the small couplings, as we have explicitly shown in Refs. [78, 79]. Further, the production cross sections at the LHC will be so small that the di-muon signal is much below the current limit [159].

3.6 Cabibbo angle anomaly

As pointed out in Refs. [160, 161], the shift of the W boson coupling to the muon could explain the recent Cabibbo angle anomaly, which may be caused by the disagreement between values V_{us} determined from beta and Kaon decays. Let us consider the observable [160]

$$R(V_{us}) := \frac{V_{us}^{K\mu}}{\sqrt{1 - |V_{ud}^\beta|^2 - |V_{ub}|^2}} = \frac{V_{us}}{\sqrt{1 - |V_{ud}/h_{\nu\mu}^L|^2 - |V_{ub}|^2}} \sim 1 + \left| \frac{V_{ud}}{V_{us}} \right|^2 \epsilon_\mu. \quad (49)$$

where $V_{us}^{K\mu}$ (V_{ud}^β) is the value of the CKM element determined from the Kaon (β) decay. The CKM elements without superscript are those in our model which are assumed to be unitary⁶. Here, $V_{us}^{K\mu} = 0.2252$ (5), $V_{ub} = 4 \times 10^{-3}$ [2] and $V_{ud} = 0.97373$ (09) [160]. The current measured value is $R(V_{us}) = 0.9891$ (27) [160]. Since $\epsilon_\mu > 0$ in this model, the tension can not be resolved by the mixing with the VL leptons. We shall not include $R(V_{us})$ in our χ^2 analysis because it can not be explained by the mixing with VL leptons, and could be explained by mixing with VL quarks.

4 Numerical results and LHC signals

4.1 χ^2 fitting

There are 12 parameters in our model,

$$x = (g', v_\Phi, m_\chi, m_L, m_E, m_N, \lambda_L, \lambda_E, \lambda_e, \lambda'_e, \lambda_n, \lambda'_n), \quad (50)$$

to be scanned in our parameter search. The SM Yukawa coupling constant y_2 is fixed to explain the muon mass for a given parameter set. We take $\lambda_N = y_n = 0$ since these are irrelevant

⁶We neglect non-unitarity of the 3×3 CKM matrix which could be induced by mixing with VL quarks, since we have shown that it is unitary up to $\mathcal{O}(10^{-11})$ for typical cases [78, 79].

Table 2: The list of observables and their values studied in our χ^2 analysis.

Obs.	Exp.	Unc.	Remark
$\Delta a_\mu \times 10^9$	2.51	0.59	Refs. [97–118]
m_W [GeV]	80.4335	0.0094	CDF value [1]
BR($W \rightarrow \mu\nu$)	0.1063	0.0015	Ref. [2]
$\Gamma(Z \rightarrow \mu\mu)$ [GeV]	0.08395	0.00018	Ref. [2]
$\Gamma(Z \rightarrow \text{inv})$ [GeV]	0.4989	0.0025	Ref. [2]
A_μ	0.142	0.015	Ref. [2]
A_{FB}^μ	0.0169	0.0013	Ref. [2]
$R_{\mu\mu}$	1.19	0.34	Ref. [2]
$R_{\gamma\gamma}$	1.10	0.07	Ref. [2]
$\Gamma(Z \rightarrow \mu\mu) / \Gamma(Z \rightarrow ee)$	1.0001	0.0024	Ref. [2]
$\Gamma(Z \rightarrow \tau\tau) / \Gamma(Z \rightarrow \mu\mu)$	1.0010	0.0026	Ref. [2]
$\Gamma(W \rightarrow \mu\nu) / \Gamma(W \rightarrow e\nu)$	0.996	0.008	Ref. [2]
$\Gamma(W \rightarrow \tau\nu) / \Gamma(W \rightarrow \mu\nu)$	1.070	0.026	Ref. [2]
$\Gamma(\tau \rightarrow \mu\nu\nu) / \Gamma(\tau \rightarrow e\nu\nu)$	0.9762	0.0028	Ref. [2]
R_{CCFR}	0.82	0.14	Ref. [150, 151]

for phenomenology after integrating out ν_R . To find points which can explain the anomalies consistently with the other observables, we minimize the χ^2 function

$$\chi^2(x) := \sum_I \frac{(y_I(x) - y_I^0)^2}{\sigma_I^2}, \quad (51)$$

where y_I 's are observables listed in Table 2. y_I^0 and σ_I are the experimental central value and its 1σ error, respectively. For R_{CCFR} , the error is chosen such that the 2σ deviation corresponds to the 95% C.L limit. Here, we assume that the W boson mass is given by the CDF result. In the SM, $\chi_{\text{SM}}^2 \simeq 94$ mainly originated from Δa_μ and m_W as well as the 2.7σ deviation in $\Gamma(W \rightarrow \tau\nu) / \Gamma(W \rightarrow \mu\nu)$.

In our analysis, we restrict the parameter space to be

$$v_\Phi \in [100, 2000] \text{ GeV}, \quad m_L, m_E \in [100, 1500] \text{ GeV}, \quad (52)$$

$$m_\chi \in [63, 1500] \text{ GeV}, \quad m_N \in [40, 1500] \text{ GeV}, \quad (53)$$

and

$$g' \in [0, 0.35], \quad \lambda_L, \lambda_E, \lambda_e, \lambda_n, \lambda'_e, \lambda'_n \in [-1, 1]. \quad (54)$$

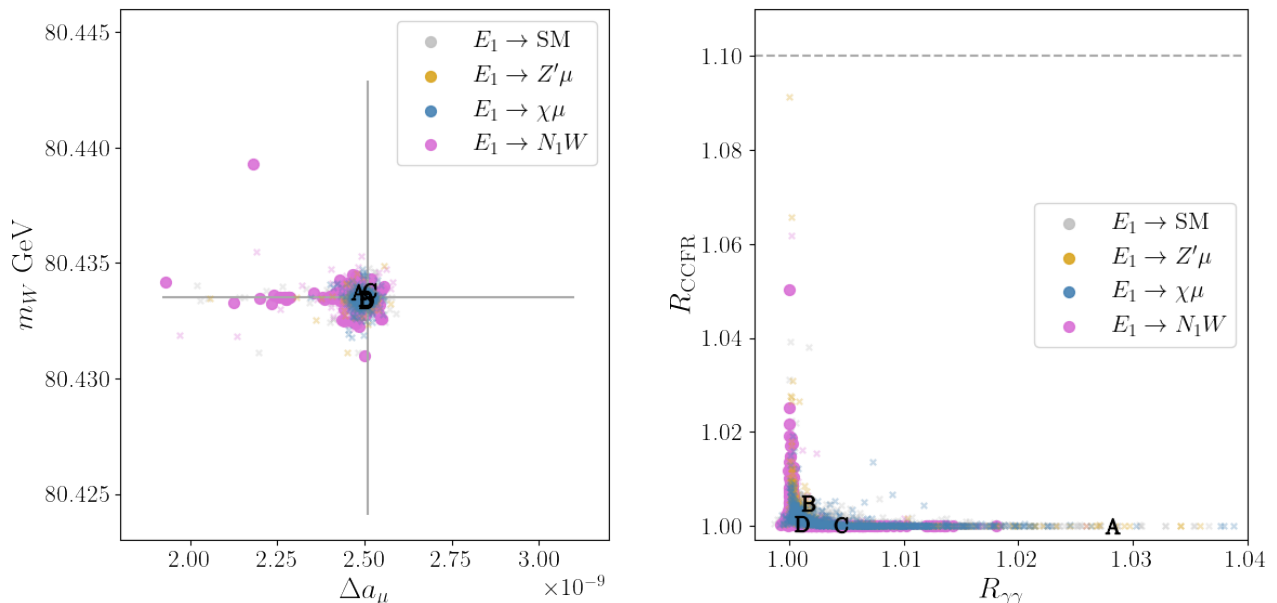


Figure 1: Scattering plots on the observables in our analysis. The cross and circle points are $100 < m_{E_1} < 175$ GeV and $m_{E_1} > 175$ GeV, respectively. All the points explain the m_W and Δa_μ within 1σ . The error bars on the left panel are the 1σ uncertainties, and the dash horizontal line on the right panel is 95% C.L. limit on R_{CCFR} . The central value of $R_\gamma = 1.10$ is outside of the figure. The benchmark points, (A), (B), (C), and (D), lie on top of each other in the left panel.

Here, the lower bounds of m_χ is chosen so that $h \rightarrow \chi\chi$ is kinematically forbidden. The $U(1)'$ gauge constant g' is required to be smaller than 0.35, so that it is perturbative up to 10^{16} GeV in the full model with VL quarks [78]. We minimize the χ^2 function from random initial points in the parameter range. We further require $m_{E_1}, m_{Z'} > 100$ GeV and $m_{N_1} > 45$ GeV for the fitted points, so that the collider limits would be avoided and $Z \rightarrow N_1 N_1$ is kinematically forbidden.

We calculated branching fractions of the Z' boson and the VL leptons. For the Z' boson decay, we calculated the two-body decays to the leptons. We neglect the decays to quarks, since the couplings to quarks will be tiny as discussed in Section 3.5. For the decays of VL leptons, we calculated the two-body decays to a SM, χ , Z' boson and a lepton. The three-body decays via off-shell Z' or W boson are calculated based on the formula shown in Appendix B if the corresponding on-shell two-body decay is kinematically forbidden.

Figures 1, 2, 3 and 4 show the scatter plots of the result of the χ^2 fitting. On these plots, the cross and circle points are $100 < m_{E_1} < 175$ GeV and $m_{E_1} > 175$ GeV, respectively. The colors of points indicate the dominant decay mode of the lightest charged VL lepton E_1 . Note that the three-body decays are also classified by its off-shell boson, e.g. $E_1 \rightarrow N_1 e \nu_e$ is a part of $E_1 \rightarrow N_1 W$ for $m_{E_1} - m_{N_1} < m_W$.

The scatter plots for the observables are shown in Fig. 1. On the left panel, the gray error bars are the 1σ errors along the axes. We see that Δa_μ and m_W are simultaneously explained on these points within 1σ . From the right panel, R_γ can deviate from unity at most 4%, and hence

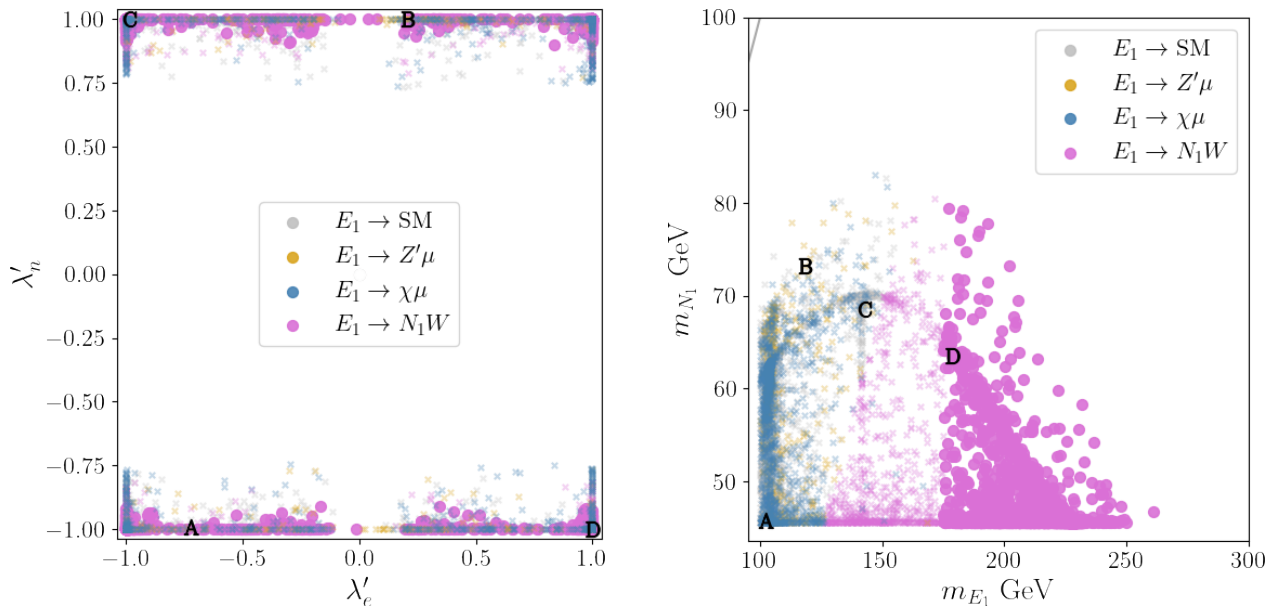


Figure 2: Scattering plots the Yukawa couplings (λ'_e, λ'_n) and the VL lepton masses (m_{E_1}, m_{N_1}). The cross and circle points are $100 < m_{E_1} < 175$ GeV and $m_{E_1} > 175$ GeV, respectively.

this is about 1σ below the experimental central value of 1.10. The neutrino trident process can be induced from the Z' boson exchange, and there are points close to the upper bound of 1.10, depicted by the gray dashed line. Altogether, all of the points explain the anomalies in m_W and Δa_μ without conflicting with the current limits on $R_{\gamma\gamma}$ and R_{CCFR} .

The left panel of Fig. 2 shows the scatter plots on (λ'_e, λ'_n) . There are points only where $|\lambda'_n| \sim 1.0$. This indicates that the mass shift of m_W is predominantly induced by the VL neutrino which can be lighter than the charged ones. The right panel shows the same plot on (m_{E_1}, m_{N_1}) . We see that the VL neutrino should be lighter than 80 GeV to explain the shift of m_W , and the upper bound becomes stronger for heavier E_1 . Thus, most of the points with $m_{E_1} > 175$ GeV have $E_1 \rightarrow N_1 W$ as the dominant decay mode.

Figure 3 shows the scatter plots on the m_{E_1} and $m_{Z'}$ (m_χ) plane on the left (right) panel. The gray line is $m_{E_1} = m_{Z'}$ or m_χ . The upper bound on $m_{Z'}$ is about 600 GeV to explain the muon $g - 2$, while χ can be much heavier. $E_1 \rightarrow N_1 W$ is the dominant decay mode even if $m_{Z'} < m_{E_1}$ due to the larger gauge coupling constant $g > g'$.

Figure 4 shows the scatter plots for the oblique parameters. The solid (dashed) lines correspond to 1σ (2σ) errors of m_W of the CDF measurement when $U = 0$ and $S = 0$ on the left and right panel, respectively. For $m_{E_1} > 175$ GeV, the points are found only around $(S, T, U) \sim (0.01, 0.15, 0.02)$, so the W boson mass shift is mainly explained by the T parameter. Different values of the oblique parameters are allowed for $m_{E_1} < 175$ GeV. These patterns of the oblique parameters will be useful to distinguish the parameter space of our model.

Tables 3 and 4 shows the benchmark points of our model. The second row of Table 4 is the SM predictions whose χ^2 value is about 94, whereas the benchmark points have $\chi^2 \sim 15$. The

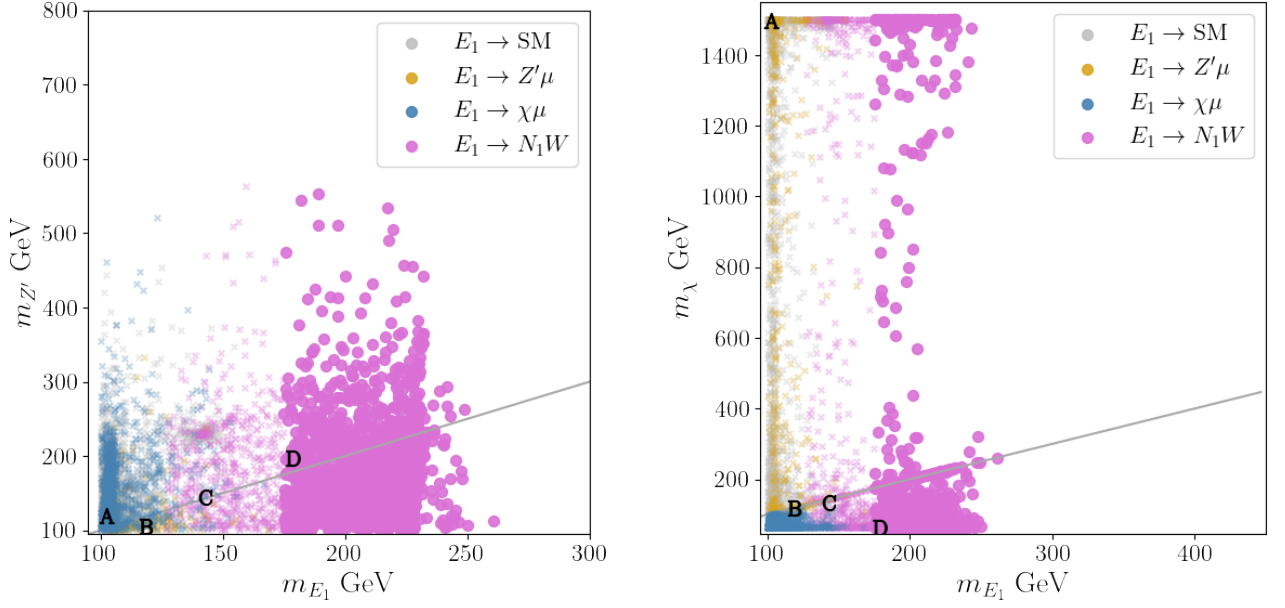


Figure 3: Scattering plots on the masses of Z' boson and the VL leptons. The cross and circle points are $100 < m_{E_1} < 175$ GeV and $m_{E_1} > 175$ GeV, respectively. The diagonal lines are respectively $m_{Z'} = m_{E_1}$ and $m_\chi = m_{E_1}$ on the left and right panel.

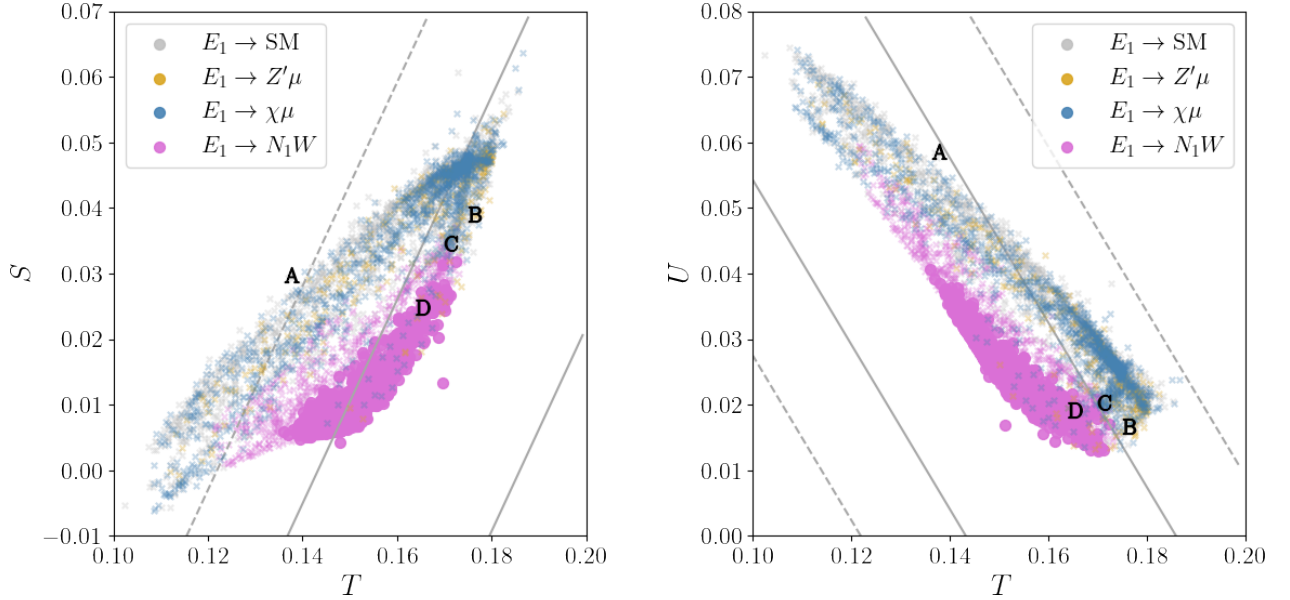


Figure 4: Scattering plots on the oblique parameters. The cross and circle points are $100 < m_{E_1} < 175$ GeV and $m_{E_1} > 175$ GeV, respectively. The solid (dashed) lines are 1σ (2σ) range of the W boson mass measured by the CDF for $U = 0$ and $S = 0$ on the left and right panel, respectively.

Table 3: Selected input parameters and branching fractions of new particles. The observables not included in our χ^2 analysis are shown in the last four rows.

benchmark	A	B	C	D
g'	0.3479	0.1212	0.3500	0.3500
$m_{Z'}$ GeV	119.2054	105.5420	145.2143	196.6287
m_χ GeV	1498.6692	118.1512	135.2181	63.1570
m_{E_1} GeV	102.2595	118.0921	142.4606	178.4233
m_{E_2} GeV	322.9197	156.0050	1524.0154	1517.7766
m_{N_1} GeV	45.8666	73.1853	68.6071	63.5020
m_{N_2} GeV	216.9324	247.9042	245.9130	258.8140
$\text{Br}(Z' \rightarrow \mu\mu)$	0.0057	0.6488	0.0017	0.0033
$\text{Br}(Z' \rightarrow \nu\nu)$	0.0000	0.1059	0.0002	0.0006
$\text{Br}(N_1 \rightarrow \chi\nu)$	0.0000	0.0000	0.0000	0.9938
$\text{Br}(N_1 \rightarrow Z'\nu)$	0.0006	0.9896	0.0027	0.0009
$\text{Br}(N_1 \rightarrow W\mu)$	0.9994	0.0104	0.9973	0.0054
$\text{Br}(E_1 \rightarrow \chi\mu)$	0.0000	0.0000	0.6454	0.0163
$\text{Br}(E_1 \rightarrow Z'\mu)$	0.0010	0.9999	0.0000	0.0000
$\text{Br}(E_1 \rightarrow WN_1)$	0.0000	0.0000	0.0000	0.9836
$\text{Br}(E_1 \rightarrow \text{SM})$	0.9990	0.0001	0.3546	0.0000
S	0.0299	0.0390	0.0347	0.0249
T	0.1377	0.1763	0.1713	0.1652
U	0.0586	0.0168	0.0204	0.0191
$R(V_{us})$	1.0002	1.0000	1.0000	1.0000

Table 4: Values of observables at the benchmark points. The second column is the SM prediction. The degree of freedom is $15 - 12 = 3$.

benchmark	SM	A	B	C	D
χ^2	93.7831	15.2403	16.2259	16.0397	16.1686
$\Delta a_\mu \times 10^9$	0.0000	2.4826	2.5001	2.5136	2.5027
m_W GeV	80.3610	80.4338	80.4335	80.4338	80.4334
$\text{Br}(W \rightarrow \mu\nu)$	0.1084	0.1084	0.1084	0.1084	0.1084
$\Gamma(Z \rightarrow \mu\mu)$	0.0840	0.0840	0.0840	0.0840	0.0840
$\Gamma(Z \rightarrow \text{inv})$	0.4976	0.4977	0.4976	0.4976	0.4976
A_μ	0.1468	0.1475	0.1468	0.1470	0.1468
A_{FB}^μ	0.0162	0.0162	0.0162	0.0162	0.0162
$R_{\mu\mu}$	1.0000	0.9277	0.9999	0.9693	0.9955
$R_{\gamma\gamma}$	1.0000	1.0282	1.0016	1.0044	1.0011
$\Gamma(Z \rightarrow \mu\mu)/\Gamma(Z \rightarrow ee)$	1.0000	0.9994	1.0000	0.9999	1.0000
$\Gamma(Z \rightarrow \tau\tau)/\Gamma(Z \rightarrow \mu\mu)$	1.0000	1.0006	1.0000	1.0001	1.0000
$\Gamma(W \rightarrow \mu\nu)/\Gamma(W \rightarrow e\nu)$	1.0000	1.0000	1.0000	1.0000	1.0000
$\Gamma(W \rightarrow \tau\nu)/\Gamma(W \rightarrow \mu\nu)$	1.0000	1.0000	1.0000	1.0000	1.0000
$\Gamma(\tau \rightarrow \mu\nu\nu)/\Gamma(\tau \rightarrow e\nu\nu)$	0.9726	0.9725	0.9726	0.9726	0.9726
R_{CCFR}	1.0000	1.0000	1.0050	1.0002	1.0004

improvement of $\chi^2 - \chi_{\text{SM}}^2 \sim 79$ is dominantly from Δa_μ and m_W . At the point (A), the Higgs boson decays can be changed by 7% and 3% in $h \rightarrow \mu\mu$ and $h \rightarrow \gamma\gamma$, respectively, due to the light VL lepton, $m_{E_1} \sim 100$ GeV. The other observables, including $\Gamma(W \rightarrow \tau\nu)/\Gamma(W \rightarrow \mu\nu)$ which gives 2.7σ , are not changed from the SM values. The values of the oblique parameters S, T, U and $R(V_{us})$ are shown in the last four rows of Table 3 for reference. We find $R(V_{us}) \gtrsim 1$ as expected from the analytical analysis.

The points (A), (B), (C) and (D) are chosen from the points whose E_1 decay is dominated by that to the SM particles, $Z'\mu$, $\chi\mu$ and N_1W , respectively. Here, the SM particles include $Z\mu, h\mu$ and $W\nu$. These points are plotted on Figs. 1, 2, 3 and 4. The branching fraction of the Z' boson to the SM leptons are shown in this table. The Z' boson will also decay to the VL leptons if it is kinematically allowed ⁷. The lightest VL neutrino N_1 decays to a SM neutrino and a χ boson if $m_\chi < m_{N_1}$ as in the point (D), while it decays to a W or Z' boson in the other cases.

4.2 LHC signals

We found that $m_{E_1} \lesssim 250$ GeV is required to explain the shift of m_W . Such a light VL lepton may be constrained by LHC searches, depending on its decay.

(A) $E_1 \rightarrow \text{SM}$

The VL lepton would decay to a SM boson and a SM lepton. If E_1 is doublet-like, the latest limit is about 1000 GeV [163] ⁸. Even for the singlet-like case, the limit is about 200 GeV [164] using the run-1 data [165]. Since E_1 is mostly doublet-like, the VL lepton lighter than 250 GeV may be excluded by the current data. However, these decay modes may be suppressed because $[g_{e_{L,R}}^Z]_{E_1\mu} = \mathcal{O}(m_\mu/m_{E_1})$, and hence the other decay mode will coexist, or even dominate the decays. Actually, $E_1 \rightarrow \text{SM}$ is sizable only on the point (A).

(B) $E_1 \rightarrow Z'\mu$

In Ref. [166], it is shown that the limit for the doublet-like VL lepton is about 500 (1200) GeV for $\text{BR}(Z' \rightarrow \mu\mu) = 2/3$ and $\text{BR}(E_1 \rightarrow Z'\mu) = 0.1$ (1.0) by the signal with four muons or more [167]. Although the Z' boson was assumed to be on-shell in Ref. [166], the limits on the VL lepton would be similar even for $m_{E_1} < m_{Z'}$. At the point (B), this decay mode dominates the others and $\text{Br}(E_1 \rightarrow Z'\mu \rightarrow \mu\mu\mu) \sim 0.65$, so this case may also be excluded.

(C) $E_1 \rightarrow \chi\mu$

This is the dominant decay mode on the point (C). This case may not be excluded if χ decays to quarks. The χ coupling to two SM fermions is induced only by the fermion mass effects, so $\chi \rightarrow bb$ can be the dominant mode ⁹. Another possibility is $\chi \rightarrow hh^*$ via the quartic

⁷Signals same as the leptonic cascade decay $Z' \rightarrow E_1\mu$ at the LHC is studied in Ref. [162]. This search could constrain our parameter space if the production cross section is sufficiently large.

⁸We consider the limit from the search for the VL lepton pair production decaying to a tau lepton as a conservative limit for our VL lepton decaying to muon.

⁹For $m_\chi > 2m_t$, $\chi \rightarrow tt$ may be the dominant decay mode, so the signal would be constrained by the 4 top quarks search [168]. Such heavy χ boson is, however, always heavier than E_1 , and $E_1 \rightarrow \chi\mu$ is kinematically forbidden.

interaction $|H|^2|\Phi|^2$ in the scalar potential. Since the decays to fermions are suppressed, this mode can dominate over the others. In this case, we expect $4h + \mu\mu$ from the E_1 pair production. Yet another possibility is loop-induced decays such as $\chi \rightarrow \gamma\gamma$ and gg , which may be particularly important for $m_\chi < m_h$. Thus there are so many decay modes that could be sizable and many parameters independent of our discussions which are involved. Thus this case may not be excluded.

(D) $E_1 \rightarrow WN_1$

This decay mode may dominate the others when $m_{N_1} < m_{E_1}$ which is favored to explain the m_W shift. The VL neutrino N_1 then decays as $N_1 \rightarrow Z'\nu$ or $N_1 \rightarrow \chi\nu$. At the point (D), $N_1 \rightarrow \chi\nu$ dominates, so the signal is $E_1E_1 \rightarrow WW + \chi\chi + \nu\nu$. This signal contains many particles in the final state, but these will be relatively soft because of the smaller phase space. Thus, there may be a case in which the point (D) is not excluded by the current bounds.

We note that the pair production of N_1 is also constrained by the $\geq 4\mu$ search [166] or the VL lepton search [163], as for E_1 pair production. Although N_1 is mostly singlet-like, there is a mixing with the doublet-like state, and thus N_1 can be pair produced from a Z boson. The light N_1 would be excluded if $\text{BR}(N_1 \rightarrow Z'\nu)$ or $\text{BR}(N_1 \rightarrow W\mu)$ is sizable. Hence, the point (C) would also be excluded by the direct N_1 search. Therefore, the benchmark points other than the point (D) may be excluded by the current data. At the point (D), the decay of χ is important for the collider signals of both N_1 and E_1 . As we have already discussed, there are various decay modes of the χ boson because of the vanishing couplings to two SM fermions, see Eq. (26), and thus there may be cases which any search can not constrain. This is an interesting subject, but is beyond the scope of this paper.

5 Summary

In this work, we studied the W boson mass in the SM extension with VL leptons and a $U(1)'$ gauge symmetry, in which only the VL leptons carry non-zero charges. The full model with VL quarks was originally considered to explain the anomalies in the muon $g - 2$ and the $b \rightarrow s\ell\ell$ decay simultaneously [78, 79]. We explicitly studied the W boson mass and Δa_μ induced by the VL leptons and the Z' boson, and we found points which can explain both anomalies. Since $b \rightarrow s\ell\ell$ can easily be explained by tiny couplings with the SM quarks, as discussed in Sec. 3.5, our model provides a simultaneous explanation for the three anomalies.

The VL leptons should be light to explain the shift of m_W . We found that the lightest charged (neutral) VL lepton E_1 (N_1) is lighter than 250 (80) GeV if absolute values of the Yukawa couplings are less than unity. In our model, the VL leptons typically decay through the Z' or χ boson. If the VL lepton decays through the Z' boson, which may decay to di-muons, there will be strong constraints from the searches for signals with four muons or more [166]. Hence, the decay to the χ boson should dominate the decay of the VL lepton, which may be achieved by the mass hierarchy $m_\chi < m_{E_1, N_1} < m_{Z'}$. The χ boson decays to the SM particles in various ways, and thus there may

be some cases for which none of the LHC searches exclude our model with the light VL leptons. Studying the decays of the χ boson in the full model with VL quarks is our future work.

Acknowledgment

The work of J.K. is supported in part by the Institute for Basic Science (IBS-R018-D1), and the Grant-in-Aid for Scientific Research from the Ministry of Education, Science, Sports and Culture (MEXT), Japan No. 18K13534. The work of S.R. is supported in part by the Department of Energy (DOE) under Award No. DE-SC0011726.

A Diagonalization of mass matrices

We first discuss the diagonalization of the charged lepton mass matrix Eq. (3). The diagonalization matrix is decomposed as

$$U_L = U_L^0 U_L^1 U_L^2, \quad U_R = U_R^0 U_R^1 U_R^2. \quad (55)$$

The unitary matrices are given by

$$U_L^0 = \begin{pmatrix} c_L & s_L & 0 \\ -s_L & c_L & 0 \\ 0 & 0 & 1 \end{pmatrix}, \quad U_R^0 = \begin{pmatrix} c_E & s_E & 0 \\ -s_E & c_E & 0 \\ 0 & 0 & 1 \end{pmatrix}, \quad (56)$$

$$U_L^1 = \begin{pmatrix} 1 - y_{42}^2 \frac{v_H^2}{2M_E^2} & y_{22}y_{24} \frac{v_H^2}{M_L^2} - y_{42}\lambda'_e \frac{v_H^2}{M_E M_L} & y_{42} \frac{v_H}{M_E} \\ -y_{22}y_{24} \frac{v_H^2}{M_L^2} + y_{42}\lambda'_e \frac{v_H^2}{M_E M_L} & 1 & 0 \\ -y_{42} \frac{v_H}{M_E} & 0 & 1 - y_{42}^2 \frac{v_H^2}{2M_E^2} \end{pmatrix} + \mathcal{O}(m_\mu^3), \quad (57)$$

$$U_R^1 = \begin{pmatrix} 1 - y_{24}^2 \frac{v_H^2}{2M_L^2} & y_{22}y_{42} \frac{v_H^2}{M_E^2} - y_{24}\lambda'_e \frac{v_H^2}{M_E M_L} & y_{24} \frac{v_H}{M_L} \\ -y_{22}y_{42} \frac{v_H^2}{M_E^2} + y_{24}\lambda'_e \frac{v_H^2}{M_E M_L} & 1 & 0 \\ -y_{24} \frac{v_H}{M_L} & 0 & 1 - y_{24}^2 \frac{v_H^2}{2M_L^2} \end{pmatrix} + \mathcal{O}(m_\mu^3), \quad (58)$$

and

$$U_L^2 = \begin{pmatrix} 1 & 0 & 0 \\ 0 & c_{eL} & -s_{eL} \\ 0 & s_{eL} & c_{eL} \end{pmatrix}, \quad U_R^2 = \begin{pmatrix} 1 & 0 & 0 \\ 0 & s_{eR} & c_{eR} \\ 0 & c_{eR} & -s_{eR} \end{pmatrix}, \quad (59)$$

where

$$\begin{pmatrix} s_{e_R} & c_{e_R} \\ c_{e_R} & -s_{e_R} \end{pmatrix} \begin{pmatrix} y_{44}v_H & M_E \\ M_L & \lambda'_e v_H \end{pmatrix} \begin{pmatrix} c_{e_L} & -s_{e_L} \\ s_{e_L} & c_{e_L} \end{pmatrix} = \text{diag}(m_{E_1}, m_{E_2}). \quad (60)$$

Here, $y_{22} = c_L c_E y_2 + s_L s_E \lambda_e$, $y_{24} = c_E s_L y_2 - s_E c_L \lambda_e$, $y_{42} = c_L s_E y_2 - c_E s_L \lambda_e$ and $y_{44} = s_L s_E y_2 + c_L c_E \lambda_e$. The unitary matrices $U_{L,R}^1$ block diagonalize the SM and VL leptons up to $\mathcal{O}(y_2^2 v_H^2)$ when we assume $\lambda_e \sim \mathcal{O}(y_2)$. These are simply identity matrices if we neglect $\mathcal{O}(m_\mu/v_\Phi)$. The unitary matrices $U_{L,R}^0$ keeps the $SU(2)_L$ gauge couplings unchanged, while $U_{L,R}^1$ do change the couplings as

$$(U_L^1)^\dagger Q_L U_L^1 = \begin{pmatrix} 1 - y_{42}^2 \frac{v_H^2}{M_E^2} & 0 & y_{42} \frac{v_H}{M_E} \\ 0 & 1 & 0 \\ y_{42} \frac{v_H}{M_E} & 0 & y_{42}^2 \frac{v_H^2}{M_E^2} \end{pmatrix}, \quad (U_R^1)^\dagger Q_R U_R^1 = \begin{pmatrix} y_{24}^2 \frac{v_H^2}{M_L^2} & 0 & -y_{24} \frac{v_H}{M_L} \\ 0 & 0 & 0 \\ -y_{24} \frac{v_H}{M_L} & 0 & 1 - y_{24}^2 \frac{v_H^2}{M_L^2} \end{pmatrix}. \quad (61)$$

For $\lambda_e v_H \lesssim m_\mu$, the correction to the muon coupling deviates from the SM value within $\mathcal{O}(10^{-6})$ for $\mathcal{O}(100)$ GeV VL lepton masses, while it can be $\mathcal{O}(1)$ for $\lambda_e \sim \mathcal{O}(1)$ with the fine-tuning for $y_{22} v_H \sim m_\mu$. Note that $U_{eL,R}^2$ does not change the SM coupling since these rotate only the VL block.

The neutrino mass matrix, Eq. (4), can be diagonalized as follows. First, we rotate \mathcal{M}_n as

$$\widetilde{\mathcal{M}}_n = \mathcal{M}_n V_L^0 = \begin{pmatrix} m_D & \cdot & \cdot \\ 0 & 0 & \widetilde{m}_N \\ 0 & \widetilde{M}_L & m_n \end{pmatrix}, \quad V_L^0 = \begin{pmatrix} 1 & 0 & 0 \\ 0 & c_N & s_N \\ 0 & -s_N & c_N \end{pmatrix} \begin{pmatrix} \tilde{c}_L & \tilde{s}_L & 0 \\ -\tilde{s}_L & \tilde{c}_L & 0 \\ 0 & 0 & 1 \end{pmatrix}, \quad (62)$$

where $m_D = \tilde{c}_L y_n v_H + \tilde{s}_L s_N \lambda_N v_\Phi$, $\widetilde{m}_N = \sqrt{m_N^2 + \lambda_n^2 v_H^2}$, $\widetilde{M}_L = c_N m_L - s_N \lambda'_n v_H$, $m_n = s_N m_L + c_N \lambda'_n v_H$ and $\widetilde{M}_L = \sqrt{\widetilde{m}_L^2 + \lambda_L^2 v_\Phi^2}$. The mixing angles are defined as

$$c_N := \frac{m_N}{\widetilde{m}_N}, \quad s_N := \frac{\lambda_n v_H}{\widetilde{m}_N}, \quad \tilde{c}_L := \frac{\widetilde{m}_L}{\widetilde{M}_L}, \quad \tilde{s}_L := \frac{\lambda_L v_\Phi}{\widetilde{M}_L}. \quad (63)$$

The dots in the first row are linear combinations of $y_n v_H$ and $\lambda_N v_\Phi$, which are irrelevant for our discussion after integrating out the right-handed neutrino ν_R . The active neutrino mass is given by m_D^2/M_R . The unitary matrices to diagonalize the neutrino mass is given by

$$U_{nL} = V_L^0 \begin{pmatrix} 1 & 0 & 0 \\ 0 & c_{nL} & -s_{nL} \\ 0 & s_{nL} & c_{nL} \end{pmatrix}, \quad U_{nR} = \begin{pmatrix} 1 & 0 & 0 \\ 0 & s_{nR} & c_{nR} \\ 0 & c_{nR} & -s_{nR} \end{pmatrix}, \quad (64)$$

up to $v_\Phi/M_R \ll 1$, where

$$\begin{pmatrix} s_{nR} & c_{nR} \\ c_{nR} & -s_{nR} \end{pmatrix} \begin{pmatrix} 0 & \widetilde{m}_N \\ \widetilde{M}_L & m_n \end{pmatrix} \begin{pmatrix} c_{nL} & -s_{nL} \\ s_{nL} & c_{nL} \end{pmatrix} = \text{diag}(m_{N_1}, m_{N_2}) \quad (65)$$

With the unitary matrix U_{n_L} , the SM muon neutrino coupling to the Z boson is rescaled as $c_L^2 + c_N^2 s_L^2$. Therefore, $s_N \sim \lambda_n v_H/m_N \ll 1$ is required for the SM-like Z boson coupling to muon neutrinos.

B Decay widths

We calculate the three-body decay, $F \rightarrow f_3 V^* \rightarrow f_3 \bar{f}_2 f_1$, of fermions via a off-shell vector boson V whose couplings are given by,

$$\mathcal{L} = V_\mu \bar{f}_1 \gamma^\mu (g_L^{12} P_L + g_R^{12} P_R) f_2 + V_\mu \bar{f}_3 \gamma^\mu (g_L^{3F} P_L + g_R^{3F} P_R) F. \quad (66)$$

The partial width is given by

$$\Gamma(F \rightarrow f_3 \bar{f}_2 f_1) = \frac{m_F}{768\pi^3} \left(|g_L^{12}|^2 + |g_R^{12}|^2 \right) \times \int_0^{(1-\sqrt{y})^2} dt \frac{\beta(t)}{(t-z)^2} \left[\left(|g_L^{3F}|^2 + |g_R^{3F}|^2 \right) \{ (1-y)^2 + (1+y)t - 2t^2 \} - 12\text{Re}(g_L^{3F} g_R^{3F*}) \sqrt{y} t \right], \quad (67)$$

where $\beta(t) = \sqrt{t^2 - 2(1+y)t + (1-y)^2}$, $y = m_3^2/m_F^2$ and $z = m_V^2/m_F^2$. Here, m_3 , m_F and m_V are respectively the masses of f_3 , F and V , and we neglect the masses of the fermions f_1 and f_2 .

References

- [1] **CDF** Collaboration, T. Aaltonen et al., *High-precision measurement of the W boson mass with the CDF II detector*, *Science* **376** (2022), no. 6589 170–176.
- [2] **Particle Data Group** Collaboration, P. A. Zyla et al., *Review of Particle Physics*, *PTEP* **2020** (2020), no. 8 083C01.
- [3] A. Strumia, *Interpreting electroweak precision data including the W -mass CDF anomaly*, [arXiv:2204.04191](#).
- [4] J. de Blas, M. Pierini, L. Reina, and L. Silvestrini, *Impact of the recent measurements of the top-quark and W -boson masses on electroweak precision fits*, [arXiv:2204.04204](#).
- [5] J. M. Yang and Y. Zhang, *Low energy SUSY confronted with new measurements of W -boson mass and muon $g-2$* , [arXiv:2204.04202](#).
- [6] G.-W. Yuan, L. Zu, L. Feng, and Y.-F. Cai, *W -boson mass anomaly: probing the models of axion-like particle, dark photon and Chameleon dark energy*, [arXiv:2204.04183](#).
- [7] P. Athron, A. Fowlie, C.-T. Lu, L. Wu, Y. Wu, and B. Zhu, *The W boson Mass and Muon $g-2$: Hadronic Uncertainties or New Physics?*, [arXiv:2204.03996](#).
- [8] C.-T. Lu, L. Wu, Y. Wu, and B. Zhu, *Electroweak Precision Fit and New Physics in light of W Boson Mass*, [arXiv:2204.03796](#).

- [9] Y.-Z. Fan, T.-P. Tang, Y.-L. S. Tsai, and L. Wu, *Inert Higgs Dark Matter for New CDF W-boson Mass and Detection Prospects*, [arXiv:2204.03693](#).
- [10] K. S. Babu, S. Jana, and V. P. K., *Correlating W-Boson Mass Shift with Muon $g - 2$ in the 2HDM*, [arXiv:2204.05303](#).
- [11] J. J. Heckman, *Extra W-Boson Mass from a D3-Brane*, [arXiv:2204.05302](#).
- [12] J. Gu, Z. Liu, T. Ma, and J. Shu, *Speculations on the W-Mass Measurement at CDF*, [arXiv:2204.05296](#).
- [13] P. Athron, M. Bach, D. H. J. Jacob, W. Kotlarski, D. Stöckinger, and A. Voigt, *Precise calculation of the W boson pole mass beyond the Standard Model with FlexibleSUSY*, [arXiv:2204.05285](#).
- [14] L. Di Luzio, R. Gröber, and P. Paradisi, *Higgs physics confronts the M_W anomaly*, [arXiv:2204.05284](#).
- [15] P. Asadi, C. Cesarotti, K. Fraser, S. Homiller, and A. Parikh, *Oblique Lessons from the W Mass Measurement at CDF II*, [arXiv:2204.05283](#).
- [16] H. Bahl, J. Braathen, and G. Weiglein, *New physics effects on the W-boson mass from a doublet extension of the SM Higgs sector*, [arXiv:2204.05269](#).
- [17] A. Paul and M. Valli, *Violation of custodial symmetry from W-boson mass measurements*, [arXiv:2204.05267](#).
- [18] E. Bagnaschi, J. Ellis, M. Madigan, K. Mimasu, V. Sanz, and T. You, *SMEFT Analysis of m_W* , [arXiv:2204.05260](#).
- [19] Y. Cheng, X.-G. He, Z.-L. Huang, and M.-W. Li, *Type-II Seesaw Triplet Scalar and Its VEV Effects on Neutrino Trident Scattering and W mass*, [arXiv:2204.05031](#).
- [20] H. M. Lee and K. Yamashita, *A Model of Vector-like Leptons for the Muon $g - 2$ and the W Boson Mass*, [arXiv:2204.05024](#).
- [21] X. Liu, S.-Y. Guo, B. Zhu, and Y. Li, *Unifying gravitational waves with W boson, FIMP dark matter, and Majorana Seesaw mechanism*, [arXiv:2204.04834](#).
- [22] J. Fan, L. Li, T. Liu, and K.-F. Lyu, *W-Boson Mass, Electroweak Precision Tests and SMEFT*, [arXiv:2204.04805](#).
- [23] K. Sakurai, F. Takahashi, and W. Yin, *Singlet extensions and W boson mass in the light of the CDF II result*, [arXiv:2204.04770](#).
- [24] R. Balkin, E. Madge, T. Menzo, G. Perez, Y. Soreq, and J. Zupan, *On the implications of positive W mass shift*, [arXiv:2204.05992](#).
- [25] T. Biekötter, S. Heinemeyer, and G. Weiglein, *Excesses in the low-mass Higgs-boson search and the W-boson mass measurement*, [arXiv:2204.05975](#).
- [26] M. Endo and S. Mishima, *New physics interpretation of W-boson mass anomaly*, [arXiv:2204.05965](#).

- [27] A. Crivellin, M. Kirk, T. Kitahara, and F. Mescia, *Correlating $t \rightarrow cZ$ to the W Mass and B Physics with Vector-Like Quarks*, arXiv:2204.05962.
- [28] Y. Heo, D.-W. Jung, and J. S. Lee, *Impact of the CDF W -mass anomaly on two Higgs doublet model*, arXiv:2204.05728.
- [29] X.-F. Han, F. Wang, L. Wang, J. M. Yang, and Y. Zhang, *A joint explanation of W -mass and muon $g-2$ in 2HDM*, arXiv:2204.06505.
- [30] Y. H. Ahn, S. K. Kang, and R. Ramos, *Implications of New CDF-II W Boson Mass on Two Higgs Doublet Model*, arXiv:2204.06485.
- [31] H. Song, W. Su, and M. Zhang, *Electroweak Phase Transition in 2HDM under Higgs, Z -pole, and W precision measurements*, arXiv:2204.05085.
- [32] M. Blennow, P. Coloma, E. Fernández-Martínez, and M. González-López, *Right-handed neutrinos and the CDF II anomaly*, arXiv:2204.04559.
- [33] G. Cacciapaglia and F. Sannino, *The W boson mass weighs in on the non-standard Higgs*, arXiv:2204.04514.
- [34] T.-P. Tang, M. Abdughani, L. Feng, Y.-L. S. Tsai, and Y.-Z. Fan, *NMSSM neutralino dark matter for W -boson mass and muon $g - 2$ and the promising prospect of direct detection*, arXiv:2204.04356.
- [35] C.-R. Zhu, M.-Y. Cui, Z.-Q. Xia, Z.-H. Yu, X. Huang, Q. Yuan, and Y. Z. Fan, *GeV antiproton/gamma-ray excesses and the W -boson mass anomaly: three faces of $\sim 60 - 70 GeV$ dark matter particle?*, arXiv:2204.03767.
- [36] M.-D. Zheng, F.-Z. Chen, and H.-H. Zhang, *The $Wl\nu$ -vertex corrections to W -boson mass in the R -parity violating MSSM*, arXiv:2204.06541.
- [37] N. V. Krasnikov, *Nonlocal generalization of the SM as an explanation of recent CDF result*, arXiv:2204.06327.
- [38] F. Arias-Aragón, E. Fernández-Martínez, M. González-López, and L. Merlo, *Dynamical Minimal Flavour Violating Inverse Seesaw*, arXiv:2204.04672.
- [39] X. K. Du, Z. Li, F. Wang, and Y. K. Zhang, *Explaining The New CDFII W -Boson Mass In The Georgi-Machacek Extension Models*, arXiv:2204.05760.
- [40] X. K. Du, Z. Li, F. Wang, and Y. K. Zhang, *Explaining The Muon $g - 2$ Anomaly and New CDF II W -Boson Mass in the Framework of (Extra)Ordinary Gauge Mediation*, arXiv:2204.04286.
- [41] J. Kawamura, S. Okawa, and Y. Omura, *W boson mass and muon $g - 2$ in a lepton portal dark matter model*, arXiv:2204.07022.
- [42] S. Kanemura and K. Yagyu, *Implication of the W boson mass anomaly at CDF II in the Higgs triplet model with a mass difference*, arXiv:2204.07511.
- [43] K. I. Nagao, T. Nomura, and H. Okada, *A model explaining the new CDF II W boson mass linking to muon $g - 2$ and dark matter*, arXiv:2204.07411.

- [44] K.-Y. Zhang and W.-Z. Feng, *Explaining W boson mass anomaly and dark matter with a $U(1)$ dark sector*, arXiv:2204.08067.
- [45] L. M. Carpenter, T. Murphy, and M. J. Smylie, *Changing patterns in electroweak precision with new color-charged states: Oblique corrections and the W boson mass*, arXiv:2204.08546.
- [46] O. Popov and R. Srivastava, *The Triplet Dirac Seesaw in the View of the Recent CDF-II W Mass Anomaly*, arXiv:2204.08568.
- [47] T. A. Chowdhury, J. Heeck, S. Saad, and A. Thapa, *W boson mass shift and muon magnetic moment in the Zee model*, arXiv:2204.08390.
- [48] D. Borah, S. Mahapatra, D. Nanda, and N. Sahu, *Type II Dirac Seesaw with Observable ΔN_{eff} in the light of W -mass Anomaly*, arXiv:2204.08266.
- [49] Y.-P. Zeng, C. Cai, Y.-H. Su, and H.-H. Zhang, *Extra boson mix with Z boson explaining the mass of W boson*, arXiv:2204.09487.
- [50] M. Du, Z. Liu, and P. Nath, *CDF W mass anomaly from a dark sector with a Stueckelberg-Higgs portal*, arXiv:2204.09024.
- [51] K. Ghorbani and P. Ghorbani, *W -Boson Mass Anomaly from Scale Invariant 2HDM*, arXiv:2204.09001.
- [52] A. Bhaskar, A. A. Madathil, T. Mandal, and S. Mitra, *Combined explanation of W -mass, muon $g - 2$, $R_{K^{(*)}}$ and $R_{D^{(*)}}$ anomalies in a singlet-triplet scalar leptoquark model*, arXiv:2204.09031.
- [53] S. Baek, *Implications of CDF W -mass and $(g - 2)_\mu$ on $U(1)_{L_\mu - L_\tau}$ model*, arXiv:2204.09585.
- [54] J. Cao, L. Meng, L. Shang, S. Wang, and B. Yang, *Interpreting the W mass anomaly in the vectorlike quark models*, arXiv:2204.09477.
- [55] D. Borah, S. Mahapatra, and N. Sahu, *Singlet-Doublet Fermion Origin of Dark Matter, Neutrino Mass and W -Mass Anomaly*, arXiv:2204.09671.
- [56] A. Batra, S. K. A., S. Mandal, and R. Srivastava, *W boson mass in Singlet-Triplet Scotogenic dark matter model*, arXiv:2204.09376.
- [57] S. Lee, K. Cheung, J. Kim, C.-T. Lu, and J. Song, *Status of the two-Higgs-doublet model in light of the CDF m_W measurement*, arXiv:2204.10338.
- [58] E. d. S. Almeida, A. Alves, O. J. P. Eboli, and M. C. Gonzalez-Garcia, *Impact of CDF-II measurement of M_W on the electroweak legacy of the LHC Run II*, arXiv:2204.10130.
- [59] Y. Cheng, X.-G. He, F. Huang, J. Sun, and Z.-P. Xing, *Dark photon kinetic mixing effects for CDF W mass excess*, arXiv:2204.10156.
- [60] J. Heeck, *W -boson mass in the triplet seesaw model*, arXiv:2204.10274.
- [61] H. Abouabid, A. Arhrib, R. Benbrik, M. Krab, and M. Ouchemhou, *Is the new CDF M_W measurement consistent with the two higgs doublet model?*, arXiv:2204.12018.

- [62] A. Batra, S. K. A, S. Mandal, H. Prajapati, and R. Srivastava, *CDF-II W Boson Mass Anomaly in the Canonical Scotogenic Neutrino-Dark Matter Model*, [arXiv:2204.11945](#).
- [63] R. Benbrik, M. Boukidi, and B. Manaut, *W-mass and 96 GeV excess in type-III 2HDM*, [arXiv:2204.11755](#).
- [64] C. Cai, D. Qiu, Y.-L. Tang, Z.-H. Yu, and H.-H. Zhang, *Corrections to electroweak precision observables from mixings of an exotic vector boson in light of the CDF W-mass anomaly*, [arXiv:2204.11570](#).
- [65] Q. Zhou and X.-F. Han, *The CDF W-mass, muon $g-2$, and dark matter in a $U(1)_{L_\mu-L_\tau}$ model with vector-like leptons*, [arXiv:2204.13027](#).
- [66] R. S. Gupta, *Running away from the T-parameter solution to the W mass anomaly*, [arXiv:2204.13690](#).
- [67] J.-W. Wang, X.-J. Bi, P.-F. Yin, and Z.-H. Yu, *Electroweak dark matter model accounting for the CDF W-mass anomaly*, [arXiv:2205.00783](#).
- [68] B. Barman, A. Das, and S. Sengupta, *New W-Boson mass in the light of doubly warped braneworld model*, [arXiv:2205.01699](#).
- [69] J. Kim, S. Lee, P. Sanyal, and J. Song, *CDF m_W and the muon $g - 2$ through the Higgs-phobic light pseudoscalar in type-X two-Higgs-doublet model*, [arXiv:2205.01701](#).
- [70] J. Kim, *Compatibility of muon $g - 2$, W mass anomaly in type-X 2HDM*, [arXiv:2205.01437](#).
- [71] R. Dcruz and A. Thapa, *W boson mass, dark matter and $(g - 2)_\ell$ in ScotoZee neutrino mass model*, [arXiv:2205.02217](#).
- [72] J. Isaacson, Y. Fu, and C. P. Yuan, *ResBos2 and the CDF W Mass Measurement*, [arXiv:2205.02788](#).
- [73] T. A. Chowdhury and S. Saad, *Leptoquark-vectorlike quark model for m_W (CDF), $(g - 2)_\mu$, $R_{K^{(*)}}$ anomalies and neutrino mass*, [arXiv:2205.03917](#).
- [74] S.-S. Kim, H. M. Lee, A. G. Menkara, and K. Yamashita, *The $SU(2)_D$ lepton portals for muon $g - 2$, W boson mass and dark matter*, [arXiv:2205.04016](#).
- [75] J. Gao, D. Liu, and K. Xie, *Understanding PDF uncertainty on the W boson mass measurements in CT18 global analysis*, [arXiv:2205.03942](#).
- [76] G. Lazarides, R. Maji, R. Roshan, and Q. Shafi, *Heavier W-boson, dark matter and gravitational waves from strings in an $SO(10)$ axion model*, [arXiv:2205.04824](#).
- [77] T.-K. Chen, C.-W. Chiang, and K. Yagyu, *Explanation of the W mass shift at CDF II in the Georgi-Machacek Model*, [arXiv:2204.12898](#).
- [78] J. Kawamura, S. Raby, and A. Trautner, *Complete vectorlike fourth family and new $U(1)'$ for muon anomalies*, *Phys. Rev. D* **100** (2019), no. 5 055030, [[arXiv:1906.11297](#)].

- [79] J. Kawamura, S. Raby, and A. Trautner, *Complete vectorlike fourth family with $U(1)'$: A global analysis*, *Phys. Rev. D* **101** (2020), no. 3 035026, [arXiv:1911.11075].
- [80] B. Allanach, F. S. Queiroz, A. Strumia, and S. Sun, *Z' models for the LHCb and $g - 2$ muon anomalies*, *Phys. Rev.* **D93** (2016), no. 5 055045, [arXiv:1511.07447]. [Erratum: *Phys. Rev.* **D95**, no. 11, 119902 (2017)].
- [81] W. Altmannshofer, M. Carena, and A. Crivellin, *$L_\mu - L_\tau$ theory of Higgs flavor violation and $(g - 2)_\mu$* , *Phys. Rev.* **D94** (2016), no. 9 095026, [arXiv:1604.08221].
- [82] E. Megias, M. Quiros, and L. Salas, *$g_\mu - 2$ from Vector-Like Leptons in Warped Space*, *JHEP* **05** (2017) 016, [arXiv:1701.05072].
- [83] S. Raby and A. Trautner, *Vectorlike chiral fourth family to explain muon anomalies*, *Phys. Rev.* **D97** (2018), no. 9 095006, [arXiv:1712.09360].
- [84] S. F. King, *Flavourful Z' models for $R_{K^{(*)}}$* , *JHEP* **08** (2017) 019, [arXiv:1706.06100].
- [85] L. Darmé, K. Kowalska, L. Roszkowski, and E. M. Sessolo, *Flavor anomalies and dark matter in SUSY with an extra $U(1)$* , *JHEP* **10** (2018) 052, [arXiv:1806.06036].
- [86] A. Crivellin, G. D'Ambrosio, and J. Heeck, *Explaining $h \rightarrow \mu^\pm \tau^\mp$, $B \rightarrow K^* \mu^+ \mu^-$ and $B \rightarrow K \mu^+ \mu^- / B \rightarrow Ke^+ e^-$ in a two-Higgs-doublet model with gauged $L_\mu - L_\tau$* , *Phys. Rev. Lett.* **114** (2015) 151801, [arXiv:1501.00993].
- [87] A. Crivellin, M. Hoferichter, and P. Schmidt-Wellenburg, *Combined explanations of $(g - 2)_{\mu,e}$ and implications for a large muon EDM*, *Phys. Rev. D* **98** (2018), no. 11 113002, [arXiv:1807.11484].
- [88] A. Crivellin, C. A. Manzari, M. Alguero, and J. Matias, *Combined Explanation of the $Z \rightarrow b\bar{b}$ Forward-Backward Asymmetry, the Cabibbo Angle Anomaly, and $\tau \rightarrow \mu\nu\nu$ and $b \rightarrow s\ell^+\ell^-$ Data*, *Phys. Rev. Lett.* **127** (2021), no. 1 011801, [arXiv:2010.14504].
- [89] A. Crivellin and M. Hoferichter, *Consequences of chirally enhanced explanations of $(g - 2)_\mu$ for $h \rightarrow \mu\mu$ and $Z \rightarrow \mu\mu$* , *JHEP* **07** (2021) 135, [arXiv:2104.03202].
- [90] M. Algueró, A. Crivellin, C. A. Manzari, and J. Matias, *Importance of $Z - Z'$ Mixing in $b \rightarrow s\ell^+\ell^-$ and the W mass*, arXiv:2201.08170.
- [91] A. Czarnecki and W. J. Marciano, *The Muon anomalous magnetic moment: A Harbinger for 'new physics'*, *Phys. Rev.* **D64** (2001) 013014, [hep-ph/0102122].
- [92] K. Kannike, M. Raidal, D. M. Straub, and A. Strumia, *Anthropic solution to the magnetic muon anomaly: the charged see-saw*, *JHEP* **02** (2012) 106, [arXiv:1111.2551]. [Erratum: *JHEP* **10**, 136 (2012)].
- [93] R. Dermisek and A. Raval, *Explanation of the Muon $g-2$ Anomaly with Vectorlike Leptons and its Implications for Higgs Decays*, *Phys. Rev.* **D88** (2013) 013017, [arXiv:1305.3522].
- [94] Z. Poh and S. Raby, *Vectorlike leptons: Muon $g-2$ anomaly, lepton flavor violation, Higgs boson decays, and lepton nonuniversality*, *Phys. Rev.* **D96** (2017), no. 1 015032, [arXiv:1705.07007].

- [95] J. Kawamura, S. Okawa, and Y. Omura, *Current status and muon $g - 2$ explanation of lepton portal dark matter*, *JHEP* **08** (2020) 042, [[arXiv:2002.12534](#)].
- [96] Y. Bai and J. Berger, *Muon $g-2$ in Lepton Portal Dark Matter*, [arXiv:2104.03301](#).
- [97] **Muon $g-2$** Collaboration, B. Abi et al., *Measurement of the Positive Muon Anomalous Magnetic Moment to 0.46 ppm*, *Phys. Rev. Lett.* **126** (2021) 141801, [[arXiv:2104.03281](#)].
- [98] **Muon $g-2$** Collaboration, G. W. Bennett et al., *Measurement of the negative muon anomalous magnetic moment to 0.7 ppm*, *Phys. Rev. Lett.* **92** (2004) 161802, [[hep-ex/0401008](#)].
- [99] T. Aoyama et al., *The anomalous magnetic moment of the muon in the Standard Model*, *Phys. Rept.* **887** (2020) 1–166, [[arXiv:2006.04822](#)].
- [100] T. Aoyama, M. Hayakawa, T. Kinoshita, and M. Nio, *Complete Tenth-Order QED Contribution to the Muon $g - 2$* , *Phys. Rev. Lett.* **109** (2012) 111808, [[arXiv:1205.5370](#)].
- [101] T. Aoyama, T. Kinoshita, and M. Nio, *Theory of the Anomalous Magnetic Moment of the Electron*, *Atoms* **7** (2019), no. 1 28.
- [102] A. Czarnecki, W. J. Marciano, and A. Vainshtein, *Refinements in electroweak contributions to the muon anomalous magnetic moment*, *Phys. Rev.* **D67** (2003) 073006, [[hep-ph/0212229](#)]. [Erratum: *Phys. Rev.* **D73**, 119901 (2006)].
- [103] C. Gnendiger, D. Stöckinger, and H. Stöckinger-Kim, *The electroweak contributions to $(g - 2)_\mu$ after the Higgs boson mass measurement*, *Phys. Rev.* **D88** (2013) 053005, [[arXiv:1306.5546](#)].
- [104] M. Davier, A. Hoecker, B. Malaescu, and Z. Zhang, *Reevaluation of the hadronic vacuum polarisation contributions to the Standard Model predictions of the muon $g - 2$ and $\alpha(m_Z^2)$ using newest hadronic cross-section data*, *Eur. Phys. J.* **C77** (2017), no. 12 827, [[arXiv:1706.09436](#)].
- [105] A. Keshavarzi, D. Nomura, and T. Teubner, *Muon $g - 2$ and $\alpha(M_Z^2)$: a new data-based analysis*, *Phys. Rev.* **D97** (2018), no. 11 114025, [[arXiv:1802.02995](#)].
- [106] G. Colangelo, M. Hoferichter, and P. Stoffer, *Two-pion contribution to hadronic vacuum polarization*, *JHEP* **02** (2019) 006, [[arXiv:1810.00007](#)].
- [107] M. Hoferichter, B.-L. Hoid, and B. Kubis, *Three-pion contribution to hadronic vacuum polarization*, *JHEP* **08** (2019) 137, [[arXiv:1907.01556](#)].
- [108] M. Davier, A. Hoecker, B. Malaescu, and Z. Zhang, *A new evaluation of the hadronic vacuum polarisation contributions to the muon anomalous magnetic moment and to $\alpha(m_Z^2)$* , *Eur. Phys. J. C* **80** (2020), no. 3 241, [[arXiv:1908.00921](#)].
- [109] A. Keshavarzi, D. Nomura, and T. Teubner, *$g - 2$ of charged leptons, $\alpha(M_Z^2)$, and the hyperfine splitting of muonium*, *Phys. Rev. D* **101** (2020), no. 1 014029, [[arXiv:1911.00367](#)].
- [110] A. Kurz, T. Liu, P. Marquard, and M. Steinhauser, *Hadronic contribution to the muon anomalous magnetic moment to next-to-next-to-leading order*, *Phys. Lett.* **B734** (2014) 144–147, [[arXiv:1403.6400](#)].

- [111] K. Melnikov and A. Vainshtein, *Hadronic light-by-light scattering contribution to the muon anomalous magnetic moment revisited*, *Phys. Rev.* **D70** (2004) 113006, [[hep-ph/0312226](#)].
- [112] P. Masjuan and P. Sánchez-Puertas, *Pseudoscalar-pole contribution to the $(g_\mu - 2)$: a rational approach*, *Phys. Rev.* **D95** (2017), no. 5 054026, [[arXiv:1701.05829](#)].
- [113] G. Colangelo, M. Hoferichter, M. Procura, and P. Stoffer, *Dispersion relation for hadronic light-by-light scattering: two-pion contributions*, *JHEP* **04** (2017) 161, [[arXiv:1702.07347](#)].
- [114] M. Hoferichter, B.-L. Hoid, B. Kubis, S. Leupold, and S. P. Schneider, *Dispersion relation for hadronic light-by-light scattering: pion pole*, *JHEP* **10** (2018) 141, [[arXiv:1808.04823](#)].
- [115] A. Gérardin, H. B. Meyer, and A. Nyffeler, *Lattice calculation of the pion transition form factor with $N_f = 2 + 1$ Wilson quarks*, *Phys. Rev.* **D100** (2019), no. 3 034520, [[arXiv:1903.09471](#)].
- [116] J. Bijnens, N. Hermansson-Truedsson, and A. Rodríguez-Sánchez, *Short-distance constraints for the $HLbL$ contribution to the muon anomalous magnetic moment*, *Phys. Lett.* **B798** (2019) 134994, [[arXiv:1908.03331](#)].
- [117] G. Colangelo, F. Hagelstein, M. Hoferichter, L. Laub, and P. Stoffer, *Longitudinal short-distance constraints for the hadronic light-by-light contribution to $(g - 2)_\mu$ with large- N_c Regge models*, *JHEP* **03** (2020) 101, [[arXiv:1910.13432](#)].
- [118] T. Blum, N. Christ, M. Hayakawa, T. Izubuchi, L. Jin, C. Jung, and C. Lehner, *The hadronic light-by-light scattering contribution to the muon anomalous magnetic moment from lattice QCD*, *Phys. Rev. Lett.* **124** (2020), no. 13 132002, [[arXiv:1911.08123](#)].
- [119] **LHCb** Collaboration, R. Aaij et al., *Test of lepton universality using $B^+ \rightarrow K^+ \ell^+ \ell^-$ decays*, *Phys. Rev. Lett.* **113** (2014) 151601, [[arXiv:1406.6482](#)].
- [120] **LHCb** Collaboration, R. Aaij et al., *Test of lepton universality with $B^0 \rightarrow K^{*0} \ell^+ \ell^-$ decays*, *JHEP* **08** (2017) 055, [[arXiv:1705.05802](#)].
- [121] **LHCb** Collaboration, R. Aaij et al., *Search for lepton-universality violation in $B^+ \rightarrow K^+ \ell^+ \ell^-$ decays*, *Phys. Rev. Lett.* **122** (2019), no. 19 191801, [[arXiv:1903.09252](#)].
- [122] **Belle** Collaboration, A. Abdesselam et al., *Test of lepton flavor universality in $B \rightarrow K^* \ell^+ \ell^-$ decays at Belle*, [arXiv:1904.02440](#).
- [123] **LHCb** Collaboration, R. Aaij et al., *Differential branching fraction and angular analysis of the decay $B_s^0 \rightarrow \phi \mu^+ \mu^-$* , *JHEP* **07** (2013) 084, [[arXiv:1305.2168](#)].
- [124] **BaBar** Collaboration, J. P. Lees et al., *Measurement of the $B \rightarrow X_s l^+ l^-$ branching fraction and search for direct CP violation from a sum of exclusive final states*, *Phys. Rev. Lett.* **112** (2014) 211802, [[arXiv:1312.5364](#)].
- [125] **LHCb** Collaboration, R. Aaij et al., *Differential branching fractions and isospin asymmetries of $B \rightarrow K^{(*)} \mu^+ \mu^-$ decays*, *JHEP* **06** (2014) 133, [[arXiv:1403.8044](#)].
- [126] **LHCb** Collaboration, R. Aaij et al., *Angular analysis and differential branching fraction of the decay $B_s^0 \rightarrow \phi \mu^+ \mu^-$* , *JHEP* **09** (2015) 179, [[arXiv:1506.08777](#)].

- [127] **LHCb** Collaboration, R. Aaij et al., *Measurement of Form-Factor-Independent Observables in the Decay $B^0 \rightarrow K^{*0} \mu^+ \mu^-$* , *Phys. Rev. Lett.* **111** (2013) 191801, [[arXiv:1308.1707](#)].
- [128] **CMS** Collaboration, V. Khachatryan et al., *Angular analysis of the decay $B^0 \rightarrow K^{*0} \mu^+ \mu^-$ from pp collisions at $\sqrt{s} = 8$ TeV*, *Phys. Lett.* **B753** (2016) 424–448, [[arXiv:1507.08126](#)].
- [129] **LHCb** Collaboration, R. Aaij et al., *Angular analysis of the $B^0 \rightarrow K^{*0} \mu^+ \mu^-$ decay using 3 fb^{-1} of integrated luminosity*, *JHEP* **02** (2016) 104, [[arXiv:1512.04442](#)].
- [130] **Belle** Collaboration, A. Abdesselam et al., *Angular analysis of $B^0 \rightarrow K^*(892)^0 \ell^+ \ell^-$* , in *Proceedings, LHCSki 2016 - A First Discussion of 13 TeV Results: Obergurgl, Austria, April 10-15, 2016*, 2016. [arXiv:1604.04042](#).
- [131] **Belle** Collaboration, S. Wehle et al., *Lepton-Flavor-Dependent Angular Analysis of $B \rightarrow K^* \ell^+ \ell^-$* , *Phys. Rev. Lett.* **118** (2017), no. 11 111801, [[arXiv:1612.05014](#)].
- [132] **ATLAS** Collaboration, T. A. collaboration, *Angular analysis of $B_d^0 \rightarrow K^* \mu^+ \mu^-$ decays in pp collisions at $\sqrt{s} = 8$ TeV with the ATLAS detector*, .
- [133] **CMS** Collaboration, C. Collaboration, *Measurement of the P_1 and P_5' angular parameters of the decay $B^0 \rightarrow K^{*0} \mu^+ \mu^-$ in proton-proton collisions at $\sqrt{s} = 8$ TeV*, .
- [134] **LHCb** Collaboration, R. Aaij et al., *Angular analysis of the $B^+ \rightarrow K^{*+} \mu^+ \mu^-$ decay*, [arXiv:2012.13241](#).
- [135] **LHCb** Collaboration, R. Aaij et al., *Test of lepton universality in beauty-quark decays*, [arXiv:2103.11769](#).
- [136] M. E. Peskin and T. Takeuchi, *A New constraint on a strongly interacting Higgs sector*, *Phys. Rev. Lett.* **65** (1990) 964–967.
- [137] M. E. Peskin and T. Takeuchi, *Estimation of oblique electroweak corrections*, *Phys. Rev. D* **46** (1992) 381–409.
- [138] L. Lavoura and J. P. Silva, *The Oblique corrections from vector - like singlet and doublet quarks*, *Phys. Rev. D* **47** (1993) 2046–2057.
- [139] I. Maksymyk, C. P. Burgess, and D. London, *Beyond S , T and U* , *Phys. Rev. D* **50** (1994) 529–535, [[hep-ph/9306267](#)].
- [140] W. Grimus, L. Lavoura, O. M. Ogreid, and P. Osland, *The Oblique parameters in multi-Higgs-doublet models*, *Nucl. Phys. B* **801** (2008) 81–96, [[arXiv:0802.4353](#)].
- [141] F. Jegerlehner and A. Nyffeler, *The Muon $g-2$* , *Phys. Rept.* **477** (2009) 1–110, [[arXiv:0902.3360](#)].
- [142] S. Antusch and V. Maurer, *Running quark and lepton parameters at various scales*, *JHEP* **11** (2013) 115, [[arXiv:1306.6879](#)].
- [143] A. Denner, *Techniques for calculation of electroweak radiative corrections at the one loop level and results for W physics at LEP-200*, *Fortsch. Phys.* **41** (1993) 307–420, [[arXiv:0709.1075](#)].

- [144] A. Djouadi, *The Anatomy of electro-weak symmetry breaking. I: The Higgs boson in the standard model*, *Phys. Rept.* **457** (2008) 1–216, [[hep-ph/0503172](#)].
- [145] W. Altmannshofer, S. Gori, M. Pospelov, and I. Yavin, *Quark flavor transitions in $L_\mu - L_\tau$ models*, *Phys. Rev.* **D89** (2014) 095033, [[arXiv:1403.1269](#)].
- [146] W. Altmannshofer, S. Gori, M. Pospelov, and I. Yavin, *Neutrino Trident Production: A Powerful Probe of New Physics with Neutrino Beams*, *Phys. Rev. Lett.* **113** (2014) 091801, [[arXiv:1406.2332](#)].
- [147] G. Magill and R. Plestid, *Neutrino Trident Production at the Intensity Frontier*, *Phys. Rev.* **D95** (2017), no. 7 073004, [[arXiv:1612.05642](#)].
- [148] S.-F. Ge, M. Lindner, and W. Rodejohann, *Atmospheric Trident Production for Probing New Physics*, *Phys. Lett.* **B772** (2017) 164–168, [[arXiv:1702.02617](#)].
- [149] P. Ballett, M. Hostert, S. Pascoli, Y. F. Perez-Gonzalez, Z. Tabrizi, and R. Zukanovich Funchal, *Neutrino Trident Scattering at Near Detectors*, *JHEP* **01** (2019) 119, [[arXiv:1807.10973](#)].
- [150] W. Altmannshofer, S. Gori, J. Martín-Albo, A. Sousa, and M. Wallbank, *Neutrino Tridents at DUNE*, [arXiv:1902.06765](#).
- [151] B. Zhou and J. F. Beacom, *Neutrino-nucleus cross sections for W -boson and trident production*, [arXiv:1910.08090](#).
- [152] J. Aebischer, W. Altmannshofer, D. Guadagnoli, M. Reboud, P. Stangl, and D. M. Straub, *B -decay discrepancies after Moriond 2019*, [arXiv:1903.10434](#).
- [153] M. Algueró, B. Capdevila, A. Crivellin, S. Descotes-Genon, P. Masjuan, J. Matias, M. Novoa Brunet, and J. Virto, *Emerging patterns of New Physics with and without Lepton Flavour Universal contributions*, *Eur. Phys. J. C* **79** (2019), no. 8 714, [[arXiv:1903.09578](#)]. [Addendum: *Eur.Phys.J.C* 80, 511 (2020)].
- [154] A. K. Alok, A. Dighe, S. Gangal, and D. Kumar, *Continuing search for new physics in $b \rightarrow s\mu\mu$ decays: two operators at a time*, [arXiv:1903.09617](#).
- [155] M. Ciuchini, A. M. Coutinho, M. Fedele, E. Franco, A. Paul, L. Silvestrini, and M. Valli, *New Physics in $b \rightarrow sl^+\ell^-$ confronts new data on Lepton Universality*, [arXiv:1903.09632](#).
- [156] A. Datta, J. Kumar, and D. London, *The B Anomalies and New Physics in $b \rightarrow se^+e^-$* , [arXiv:1903.10086](#).
- [157] K. Kowalska, D. Kumar, and E. M. Sessolo, *Implications for New Physics in $b \rightarrow s\mu\mu$ transitions after recent measurements by Belle and LHCb*, [arXiv:1903.10932](#).
- [158] A. Arbey, T. Hurth, F. Mahmoudi, D. Martinez Santos, and S. Neshatpour, *Update on the $b \rightarrow s$ anomalies*, [arXiv:1904.08399](#).
- [159] **ATLAS** Collaboration, G. Aad et al., *Search for high-mass dilepton resonances using 139 fb⁻¹ of pp collision data collected at $\sqrt{s} = 13$ TeV with the ATLAS detector*, *Phys. Lett. B* **796** (2019) 68–87, [[arXiv:1903.06248](#)].

- [160] M. Kirk, *Cabibbo anomaly versus electroweak precision tests: An exploration of extensions of the Standard Model*, *Phys. Rev. D* **103** (2021), no. 3 035004, [arXiv:2008.03261].
- [161] A. Crivellin, F. Kirk, C. A. Manzari, and M. Montull, *Global Electroweak Fit and Vector-Like Leptons in Light of the Cabibbo Angle Anomaly*, *JHEP* **12** (2020) 166, [arXiv:2008.01113].
- [162] R. Dermisek, J. Kawamura, E. Lunghi, N. McGinnis, and S. Shin, *Leptonic cascade decays of a heavy Higgs boson through vectorlike leptons at the LHC*, arXiv:2204.13272.
- [163] **CMS** Collaboration, A. Tumasyan et al., *Inclusive nonresonant multilepton probes of new phenomena at $\sqrt{s} = 13$ TeV*, arXiv:2202.08676.
- [164] R. Dermisek, J. P. Hall, E. Lunghi, and S. Shin, *Limits on Vectorlike Leptons from Searches for Anomalous Production of Multi-Lepton Events*, *JHEP* **12** (2014) 013, [arXiv:1408.3123].
- [165] *Search for New Physics in Events with Three Charged Leptons with the ATLAS detector*, tech. rep., CERN, Geneva, Jul, 2013. All figures including auxiliary figures are available at <https://atlas.web.cern.ch/Atlas/GROUPS/PHYSICS/CONFNOTES/ATLAS-CONF-2013-070>.
- [166] J. Kawamura and S. Raby, *Signal of four muons or more from a vector-like lepton decaying to a muon-philic Z' boson at the LHC*, *Phys. Rev. D* **104** (2021), no. 3 035007, [arXiv:2104.04461].
- [167] **ATLAS** Collaboration, G. Aad et al., *Search for supersymmetry in events with four or more charged leptons in 139 fb^{-1} of $\sqrt{s} = 13$ TeV pp collisions with the ATLAS detector*, *JHEP* **07** (2021) 167, [arXiv:2103.11684].
- [168] **ATLAS** Collaboration, M. Aaboud et al., *Search for four-top-quark production in the single-lepton and opposite-sign dilepton final states in pp collisions at $\sqrt{s} = 13$ TeV with the ATLAS detector*, *Phys. Rev. D* **99** (2019), no. 5 052009, [arXiv:1811.02305].